Seminars in Cell and Developmental Biology 121 (2022) 99–113

Contents lists available at ScienceDirect

Seminars in Cell and Developmental Biology

journal homepage: www.elsevier.com/locate/semcdb

Review

Planar cell polarity (PCP) proteins support spermatogenesis through cytoskeletal organization in the testis☆

Lingling Wang [a,b], Tiao Bu [b], Linxi Li [a], Xiaolong Wu [b], Chris K.C. Wong [c], Adolfo Perrotta [d], Bruno Silvestrini [e], Fei Sun [b], C. Yan Cheng [a,*]

[a] The Second Affiliated Hospital and Yuying Children's Hospital, Wenzhou Medical University, Wenzhou, Zhejiang 325027, China
[b] Institute of Reproductive Medicine, Nantong University School of Medicine, Nantong, Jiangsu 226001, China
[c] Department of Biology, Hong Kong Baptist University, Kowloon, Hong Kong, China
[d] Department of Translational & Precision Medicine, Sapienza University of Rome, Rome 00185, Italy
[e] The Noopolis Foundation, Via Domenico Tardini 35, Rome 00167, Italy

ARTICLE INFO

Keywords:
Testis
Spermatogenesis
PCP proteins
Sertoli cells
Cytoskeletons
F-actin
Microtubules

ABSTRACT

Few reports are found in the literature regarding the role of planar cell polarity (PCP) in supporting spermatogenesis in the testis. Yet morphological studies reported decades earlier have illustrated the directional alignment of polarized developing spermatids, most notably step 17–19 spermatids in stage V-early VIII tubules in the testis, across the plane of the epithelium in seminiferous tubules of adult rats. Such morphological features have unequivocally demonstrated the presence of PCP in developing spermatids, analogous to the PCP noted in hair cells of the cochlea in mammals. Emerging evidence in recent years has shown that Sertoli and germ cells express numerous PCP proteins, mostly notably, the core PCP proteins, PCP effectors and PCP signaling proteins. In this review, we discuss recent findings in the field regarding the two core PCP protein complexes, namely the Van Gogh-like 2 (Vangl2)/Prickle (Pk) complex and the Frizzled (Fzd)/Dishevelled (Dvl) complex. These findings have illustrated that these PCP proteins exert their regulatory role to support spermatogenesis through changes in the organization of actin and microtubule (MT) cytoskeletons in Sertoli cells. For instance, these PCP proteins confer PCP to developing spermatids. As such, developing haploid spermatids can be aligned and orderly packed within the limited space of the seminiferous tubules in the testes for the production of sperm via spermatogenesis. Thus, each adult male in the mouse, rat or human can produce an upward of 30, 50 or 300 million spermatozoa on a daily basis, respectively, throughout the adulthood. We also highlight critical areas of research that deserve attention in future studies. We also provide a hypothetical model by which PCP proteins support spermatogenesis based on recent studies in the testis. It is conceivable that the hypothetical model shown here will be updated as more data become available in future years, but this information can serve as the framework by investigators to unravel the role of PCP in spermatogenesis.

Abbreviations: Arp2/3, actin-related protein2/3; BTB, Blood-testis barrier; *Celsr*, cadherin, EGF LAG seven-pass G-type receptor; Dsh, Dishevelled (in *Drosophila*); Dvl, segment polarity protein dishevelled homolog (in vertebrates); *Dvl1*, dishevelled segment polarity protein 1; Dgo, Diego (in *Drosophila*); Ds, Dachsous (in *Drosophila*); Dchs, Dachsous cadherin-related protein (in vertebrates); ES, Ectoplasmic specialization; Eps8, epidermal growth factor receptor pathway substrate 8; Fz, Frizzled (in *Drosophila*); Fzd, Frizzled (in vertebrates); Fzd1, frizzled class receptor 1; Ft, Fat (in *Drosophila*); *Fat1*, FAT atypical cadherin 1 (in vertebrates); Fj, Four-Jointed (in *Drosophila*); *Fjx1*, four-jointed box kinase 1 (in vertebrates); Fmi, Flamingo; Fw, Furrowed; Invs, Inversin; Mwh, Multiple wing hairs; MT, microtubule; MARK, microtubule affinity regulating kinase 2; MAPs, microtubule associated proteins; MAP1a, microtubule associated protein 1a; PKCζ, atypical protein kinase Cζ; PCP, planar cell polarity; Pk, Prickle; Pk1, Prickle1; *Prickle1*, prickle planar cell polarity protein 1; Stbm, Strabismus; Stan, Starry Nigh; TJ, Tight junction; TM, Transmembrane; Vang, Van Gogh; Vangl, Van Gogh-like; Vangl1, Van Gogh-like 1; ZO-1, Zonula occludens-1.

☆ This work was supported in part by grants from the National Key Research and Development Program of China (2018YFC1003500 to S.F.), the National Natural Science Foundation of China (NSFC) (81971367 to L.L.), the Wenzhou Science & Technology Bureau (Y20190015 to L.L.), the China Shenzhen Science Technology and Innovative Commission (SZSTI) (SZSTIJCYJ20180508152336419 to C.K.C.W), and the Second Affiliated Hospital & Yuying Children's Hospital of Wenzhou Medical University (to C.Y.C.). L.W. was supported by a China Pharmaceutical University World Explorer Study Abroad Scholarship.

* Corresponding author.
E-mail address: yancheng01@aol.com (C.Y. Cheng).

https://doi.org/10.1016/j.semcdb.2021.04.008
Received 3 February 2021; Received in revised form 31 March 2021; Accepted 6 April 2021
Available online 29 May 2021

1. Introduction

Planar cell polarity (PCP), or tissue polarity, refers to the directional alignment of polarized cells across the plane of an epithelium [1–3], such as steps 17–19 spermatids in stage V-VIII tubules of the rat testis [4]. Other notable examples of PCP structures in vertebrates such as rodents and humans are hair cells in the cochlea, cilia that mediate convection currents in the oviduct, and feathers or fur in the epidermis; but also the bristles that cover the insect body, and *Drosophila* pupal wing epithelium [5–9]. PCP is also crucial to support collective cell movements during tissue morphogenesis, such as gastrulation and axis elongation for convergent extension during embryonic development. On the other hand, PCP transmits directional and signaling information across the tissue plane so that groups of cells can migrate coordinately along a common axis, generally orthogonal to the apico-basal axis [10–13].

During spermatogenesis, most notably spermiogenesis, developing spermatids at stages V-VIII of the epithelial cycle in rodent testes, groups of polarized elongating/elongated spermatids (with their heads aligned to the basement membrane but tails pointed to the seminiferous tubule lumen, displaying head-to-tail apico-basal polarity) are directionally aligned across the plane of the seminiferous epithelium [4,14], displaying PCP. On the other hand, elongate spermatids are being transported either toward the tubule lumen (in stages VI-VIII tubules) or toward the basement membrane (at stage IV-V of the cycle) [15–17]. These morphological features have been demonstrated in 3 dimensional (3D)-constructed images by confocal microscopy [18]. Subsequent biochemical and molecular studies have also demonstrated unequivocally the significance of spermatid PCP [15]. For instance, a knockdown of PCP protein Vangl2 (Van Gogh-like 2) (Table 1) by RNAi in the testis in vivo led to considerable loss of spermatid PCP wherein elongated spermatid alignment was in disarray, impeding spermatid adhesion and apico-basal polarity, but also perturbing intracellular protein trafficking due to defects in the actin and microtubule (MT) cytoskeletons [15,18]. It is likely that such defects in cytoskeletons following Vangl2 knockdown (KD) perturb proper transport of nutrients to developing spermatids, but also removal of unwanted cellular components such as residual bodies and phagosomes through intracellular degradation to maintain seminiferous epithelial homeostasis.

Earlier genetic studies in *Drosophila* [19] and recent studies in the rat testis [15,18] have identified several PCP core proteins and protein complexes as follows (Table 1). In order to simplify discussion, we only refer to the vertebrate orthologs of PCP proteins here unless otherwise specified since the corresponding *Drosophila* proteins are noted in Table 1. (i) The four-pass transmembrane proteins, namely Van Gogh-like 1 (Vangl1) and Vangl2, are the vertebrate orthologs of Vang. In rat testis, the Vangl2 integral membrane protein forms a complex with Prickle (Pk) which is the cytoplasmic adaptor/scaffold protein(s). Three Prickle orthologs in vertebrates are known to date namely Pk1, Pk2 and Pk3. (ii) Ten seven-pass transmembrane proteins called Frizzled (Fzd), from Fzd1 to Fzd10 are known. Each Fzd in vertebrates, such as in rat testes, bind to the cytoplasmic adaptor/scaffold proteins Dishevelled (Dvl1, 2 or 3), Diversin and/or Inversin to form a protein complex. (iii) Three seven-pass transmembrane proteins Celsr1, Celsr2 and Celsr3 are expressed in the testis. (iv) A single-pass transmembrane protein Furrowed (Fw) is noted in *Drosophila* but its vertebrate ortholog has not been identified. At present, the adaptor/scaffold protein(s) for Celsr in vertebrates are not known. Studies in *Drosophila* have shown that both Fmi and Fw are crucial to support the intercellular interactions of Fz and Vang to maintain the corresponding function of Fz and Vang to support PCP in *Drosophila* [20] (Fig. 1). Additionally, there are three other transmembrane proteins in the Fat/Dchs/Fjx1 Pathway comprised of Fat (Fat1, 2, 3 and 4), Dchs (Dchs1 and Dchs2) and Fjx1 (Table 1). The function of this group of PCP proteins in the testis remains to be investigated. Studies have shown that Prickle [21,22] is working in concert with Vangl2 to create the Vangl2/Pk protein complex to modulate PCP function through multiple wing hairs (Mwh) [23] to regulate actin and/or microtubule (MT) cytoskeletal function [24–26] in *Drosophila*. Interestingly, recent studies in the testis have shown that Vangl2 [15,18] exert its effects to modulate spermatid PCP, through the PKCζ and MARK2 signaling pathway [18], which in turn affect the actin- and MT-based cytoskeletal organization across the seminiferous epithelium. On the other hand, Dvl3 also exerts its regulatory effects to modulate spermatid PCP function in the testis through the actin and MT cytoskeletons in the testis [27]. Collectively, these findings have shown that PCP proteins, similar to the cell polarity complexes, exert their regulatory effects through their actions on cytoskeletal organization [28,29]. In this review, we critically evaluate recent findings in the testis, and to provide a hypothetical model regarding the role of PCP proteins in spermatogenesis. It is conceivable that this model will be modified in the years to come when more data are available. We also highlight some much needed studies in the testis in order to unravel the physiological function of PCP proteins in the biology of spermatogenesis.

Table 1
Planar cell polarity (PCP) proteins in *Drosophila* and their orthologs in mammals.

Drosophila PCP proteins	Symbol (in *Drosophila*)	Mammalian PCP protein orthologs	Symbol (in mammals; including different isoforms)
Core Pathway			
Strabismus/ Van Gogh	**Stbm/Vang**	**Van Gogh-like**	**Vangl (Vangl1, Vangl2)**
Prickle	Pk	Prickle	Pk (Pk1, Pk2, Pk3)
Frizzled	**Fz**	**Frizzled class receptor**	**Fz/Fzd (Fzd1 to 10)**
Dishevelled	Dsh	Dishevelled	Dvl (Dvl1, Dvl2, Dvl3)
Diego	Dgo	Inversin Diversin	Invs Diversin (Ankrd6)
Flamingo/ Starry Night	**Fmi/Stan**	**Cadherin, EGF LAG seven-pass G-type receptor**	**Celsr (Celsr1, Celsr2, Celsr3)**
Furrowed	**Fw**	—	—
Ft/Ds/Fj Pathway			
Fat	**Ft**	**Fat atypical cadherin**	**Fat (Fat1, Fat2, Fat3, Fat4)**
Dachsous	**Ds**	**Dachsous**	**Dchs (Dchs1, Dchs2)**
Four-Jointed	**Fj**	**Four-jointed box kinase1**	**Fjx1**

All the PCP proteins listed above are integral membrane proteins (boldfaced) including the corresponding orthologs in rodents/humans which can be classified into two pathways of either the Core Pathway or the Ft/Ds/Fj Pathway. Except for Prickle, Dishevelled and Diego, which are adaptor proteins and cytosolic proteins that form a functional complex with the corresponding integral membrane proteins.

2. PCP proteins in the testis

At the cellular and molecular level, planar cell polarity (PCP) is conferred by intercellular protein complexes between adjacent cells with distinctively different heterologous components, which, in turn, are regulated by two discrete pathways: namely the Core Planar Polarity pathway [2,30] and the Fat/Dachsous/Four-Jointed box kinase 1 (Fat/Dchs/Fjxt) pathway [31,32] (Table 1, Fig. 1). Based on studies in cells of *Drosophila* and insects, and in hair cells of rodents and humans, alignment of core PCP proteins are either axial (or bipolar) asymmetric or vectorial (or unipolar) asymmetric [5,25] (Fig. 1). Axial asymmetry is conferred by transmembrane proteins Celsr (e.g., Celsr1, Celsr2, Celsr3) in vertebrates [known as Flamingo, Fmi, also called Starry Night (Stan), in *Drosophila*], and also Furrowed (Fw, a *Drosophila* selectin family member but its ortholog in vertebrate is not yet known) (Fig. 1). The intercellular Celsr- and Fw-based interacting proteins localize to both poles along one planar axis (Fig. 1; Table 1) wherein Fw forms

homophilic cell-adhesion intercellular bridges to mediate Fzd-Vangl2 intercellular interactions, analogous to Fmi which also facilitates Fzd-Vangl2 interactions between cells [5,25] (Fig. 2). On the other hand, vectorial asymmetry is conferred by transmembrane proteins Fzd and Vangl in vertebrates (e.g., Vangl1, Vangl2) in which they localize to one pole of each cell preferentially to create the intercellular protein complex but not adjacent to one another (Fig. 1, Table 1) [5,25]. Diego [Dgo in *Drosophila* and its ortholog in vertebrate is comprised of two proteins known as Diversin and Inversin (Invs)] and Dishevelled (Dsh in *Drosophila* vs. Dvl in vertebrates including Dvl1, Dvl2, Dvl3) are the cytoplasmic adaptor protein of Fzd, whereas Prickle (Pk in *Drosophila* vs. Pk1, Pk2 in vertebrates) is the cytoplasmic adaptor protein of Vangl2. Fzd/Invs/Dvl and Vangl2/Pk also activate different downstream signaling pathway and their cellular distribution are mutually exclusive, but they work in concert to maintain vectorial asymmetry through their differential action on actin cytoskeleton (Fig. 1). For instance, the Vangl2/Pk complex exerts its effects downstream through Mwh (multiple wing hairs, a PCP effector molecule [33], but its vertebrate ortholog is not known) [23] to inhibit F-actin polymerization. On the other hand, the Fz/Dgo/Dsh complex promotes polymerization of actin microfilaments through Rho-family GTPases and other effector proteins (e.g., ROK, Rho-associated kinase) [5,25,34,35] (Fig. 1). Additionally, components of the core planar polarity proteins can interact with each other. For instance, Vangl2 is known to interact with Fzd3 [36], Celsr1 [37] and Dvl3 [38].

In the Fat/Dachsous/Four-Jointed (Ft/Ds/Fj) pathway, the atypical cadherins Fat and Dachsous (Dchs) are both single-pass transmembrane proteins, which create an cell adhesion complex with Four-Jointed Box Kinase 1 (Fjx1) [3,31,32] (Fig. 2). Fjx1 is a type II transmembrane protein with a single transmembrane span and a protein kinase catalytic domain, capable of phosphorylating Fat and Dchs. When Fat is phosphorylated by Fjx1, Fat binds better to the cadherin Dchs by creating a strong adhesive protein complex of Fjx1/Dchs between adjacent cells, but when Dchs is phosphorylated, it has a reduced affinity for binding to Fjx1 [39–41] (Fig. 2). As such, Fjx1 is a crucial modulator of the Fat/Dchs adhesive activity, which in turn, also modulates the intercellular complexes of Fz/Dsh/Dgo and Vangl/Pk. In brief, Ft and Ds are phosphorylated by the protein kinase Fx1j, but with opposing effects on their heterophilic binding affinities. On the other hand, Dchs (e.g., Dchs1, Dchs2) and Fat proteins (e.g., Fat1, 2, 3 and 4) function as ligand and receptor, respectively, for the intercellular signaling pathway that regulates Hippo signaling to support PCP, which is essential to support

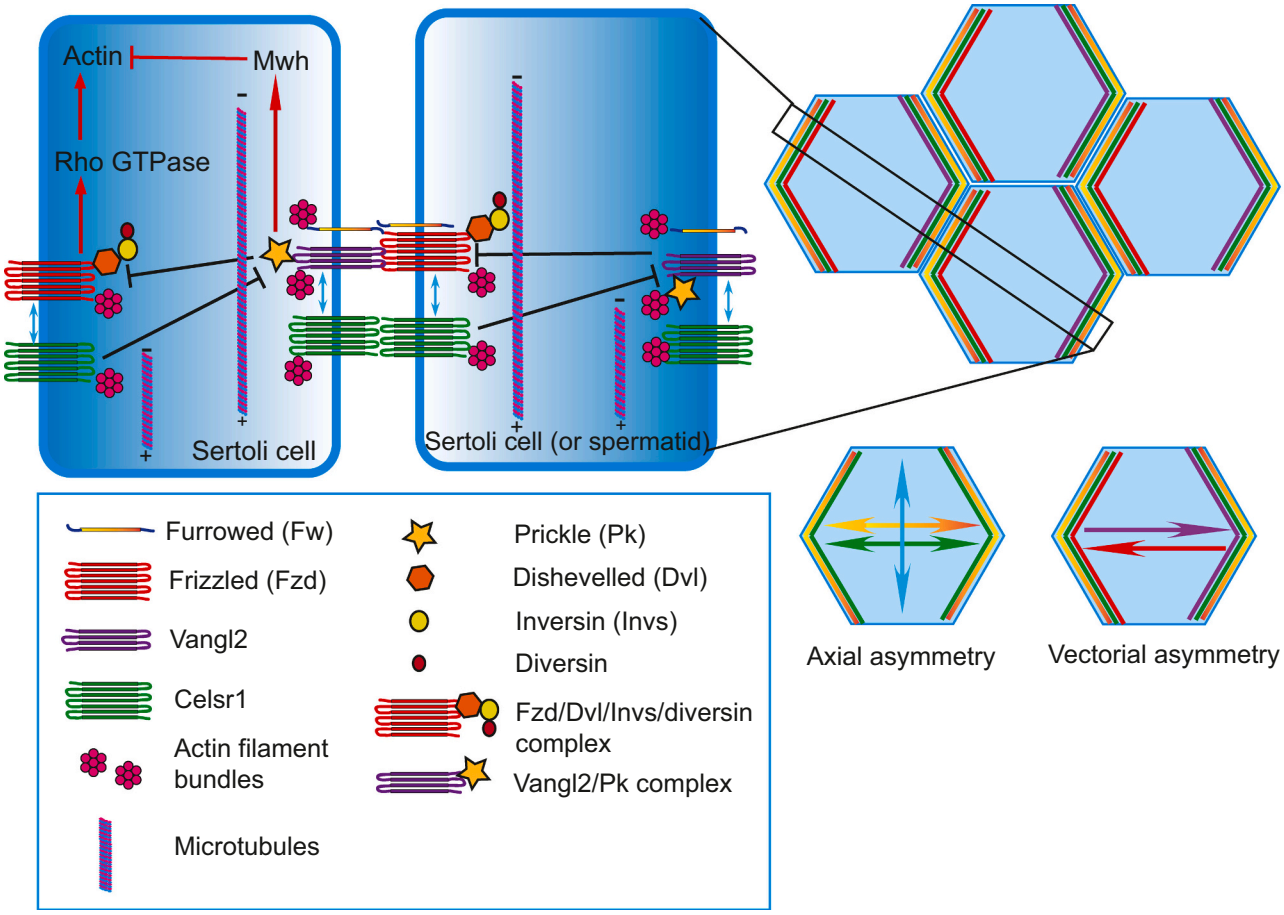

Fig. 1. Asymmetric distribution of core PCP proteins. Asymmetric distribution of core PCP proteins support orientation of cuticular hair in hair cells in *Drosophila* (*right* panel). However, this asymmetric distribution of core PCP proteins is also applicable to Sertoli cells (i.e., Sertoli-Sertoli cell interface) and developing spermatids (i.e., Sertoli cell-elongate spermatid interface) in the testis to support spermatid and Sertoli cell PCP during the epithelial cycle of spermatogenesis (*left* panel). Core PCP proteins, namely Vangl2/Prickle (Pk) protein complex and Frizzled (Fzd)/Dishevelled (Dvl)/Inversin (Invs)/Diversin protein complex, adopt vectorial asymmetries where each protein complex localizes to opposite poles of the cell; and do not form homophilic intercellular bridges. On the other hand, Celsr1 (or Fw) displays axial asymmetry where it localizes to intercellular junctions via homophilic intercellular bridges and oriented along one tissue axis. However, it is established in *Drosophila* that Celsr (or Fw) that forms homophilic intercellular bridges of Celsr-Celsr (or Fw-Fw) to mediate and/or stabilize Fzd-Vangl2 interaction. For the testis, it is likely that Celsr-Celsr intercellular cell junction is sufficient to confer stabilization of the Vangl2/Fzd interactions to confer PCP in spermatids and Sertoli cells since Fw remains to be identified in the testis or tissues/organs in mammals. For the *left* panel, it is noted that if the cell on the right side is an elongated spermatid, the actin filament bundles and microtubule cytoskeleton are absent since elongated spermatids have virtually no cytosol, but components of the Vangl2/Pk and Fzd/Dvl protein complexes have been identified in these germ cells [15,18,27].

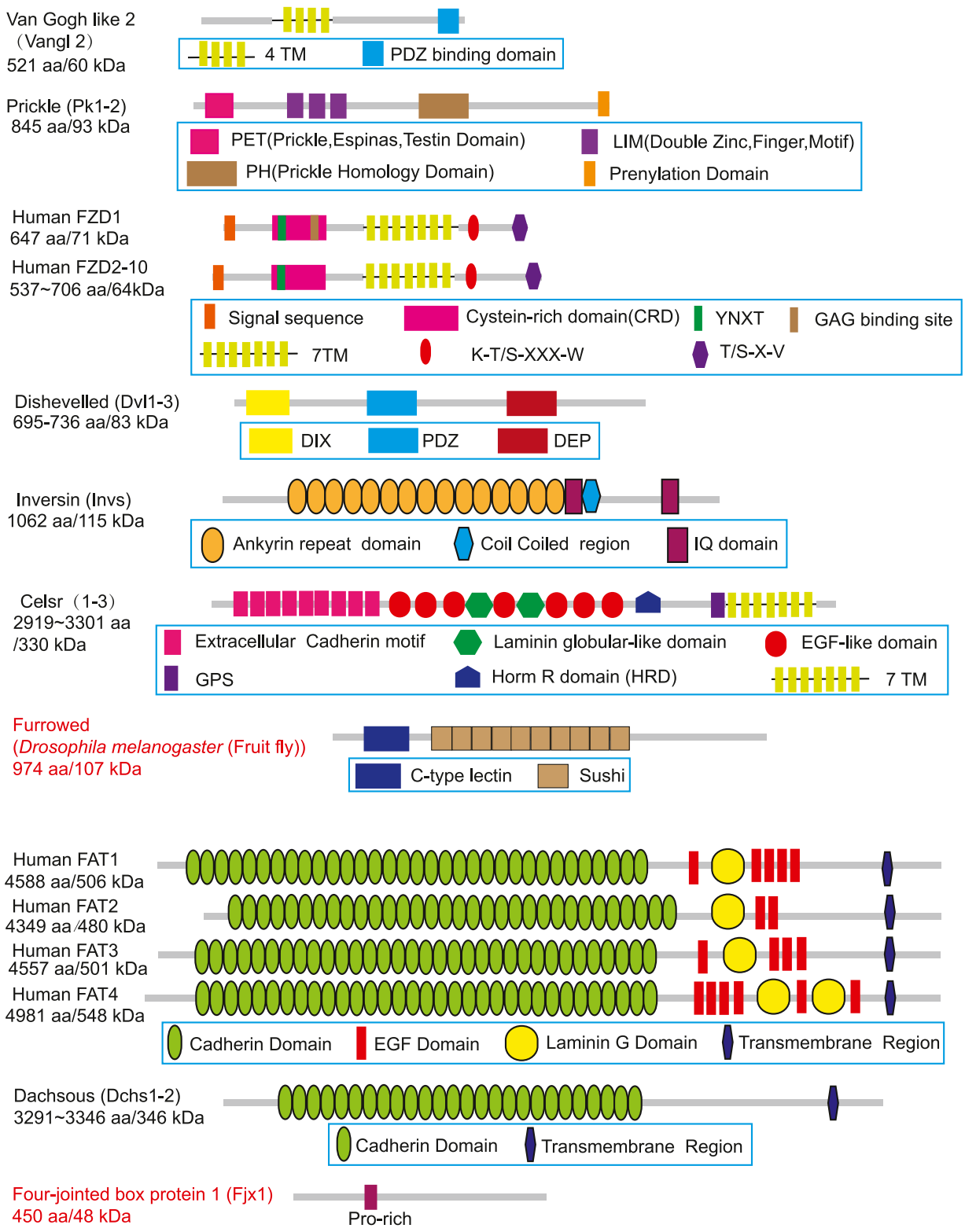

Fig. 2. Functional domains of the component proteins of the PCP Core Pathway protein complexes and Fat/Dchs/Fjx1 Pathway protein complex. For all the PCP proteins shown here, the NH_2-terminus is oriented on the *left* and the COOH-terminus is on the *right*. As noted in Table 1, the Core PCP protein complexes are: Vangl1/Pk or Vangl2/Pk complex, Fzd/Dvl/Invs/Diversin (Ankrd6) complex which are known to form intercellular junction complexes via heterophilic intercellular bridges of Vangl2/Pk-Fzd/Dvl/Invs/Diversin. These PCP intercellular junctions as noted in Fig. 1 are supported by Celsr-Celsr (and Fw-Fw) homophilic cell adhesion intercellular bridges. The role of Fat/Dchs/Fjx1 complex in the testis remains to be investigated. Nonetheless, studies in *Drosophila* have shown that Fat and Dchs are transmembrane protocadherins that localize to opposite sides of the cell where they form intercellular heterodimeric adhesion bridges between adjacent cells [88–90]. The Fat/Dchs interaction is regulated by the cytoplasmic Fj, a Golgi-associated protein kinase, capable of phosphorylating Fat and Dchs, thereby modulating their binding affinity [39,40,91]. On this note, it is noteworthy that except Fw, all the components of the two PCP Pathways have been identified in the testis including components of the Fat/Dchs/Fjx1 complex, even though detailed investigations have only been conducted on the Vangl2/Pk and Fzd/Dvl complexes.

Table 2
Phenotypes of genetic models following KO of PCP proteins in mice.

Gene	Study model	Phenotypes
Fzd1	*Fz1*$^{-/-}$	*Fz1*$^{-/-}$ mice were healthy and fertile, without notable developmental defects [92].
Fzd2	*Fz2*$^{-/-}$	50% of *Fz2*$^{-/-}$ mice had a cleft palate and died at neonatal age, the other ~50% that survived had variable degree of runting during development [92].
	Fz1$^{-/-}$; *Fz2*$^{-/-}$	Cardiac defects in *Fz1*$^{-/-}$;*Fz2*$^{-/-}$ embryos [92].
	Fz1$^{+/-}$;*Vangl2*$^{lp/+}$, *Fz2*$^{+/-}$;*Vangl2*$^{lp/+}$, *Fz1*$^{+/-}$;*Fz2*$^{+/-}$; *Vangl2*$^{lp/+}$, *Fz2*$^{-/-}$;*Vangl2*$^{lp/+}$	Neural tube defects (NTDs) [92].
Fzd3	*Fz3*$^{-/-}$	Defects in axonal development and pathfinding in the CNS [93,94].
	Fz3$^{-/-}$; *Fz6*$^{-/-}$	*Fz3*$^{-/-}$; *Fz6*$^{-/-}$ embryos had defects in neural tube formation and died shortly after birth [95].
Fzd4	*Fz4*$^{-/-}$	Progressive cerebellar, auditory, and esophageal dysfunction [96]; defects in inner ear development and defects of the retinal vasculature [97].
Fzd5	*Fzd5* $^{-/-}$, *Fzd5* $^{+/-}$	Heterozygotes were viable, fertile and appeared normal, homozygous embryos died *in utero* around 10.75 days post coitum, owing to defects in yolk sac angiogenesis; loss of *Fz5* also produces defects in placental angiogenesis [98].
Fzd6	*Fz6*$^{-/-}$	In *Fz6*$^{-/-}$ mice, global orientation of hair follicles was disrupted, leading to waves, whorls, and tufts [99].
Fzd7	*Fz7*$^{-/-}$	Fz7$^{(-/-)}$ mice had tail truncation and kinking with 100% penetrance and ventricular septal defects (VSDs) with ~15% penetrance [100].
	Fz2$^{-/-}$; *Fz7*$^{-/-}$	*Fz2(-/-); Fz7(-/-)* mice exhibit convergent extension defects and mid-gestational lethality with 100% penetrance [100].
Fzd8	*Fzd8*$^{-/-}$	Fzd8-deficient mice had defects in bone development [101].
Fzd9	*Fzd9*$^{-/-}$	Fzd9$^{-/-}$ mice had low bone mass due to defects in bone formation [102]; abnormal B-cell development [103]; mice had normal gross anatomical hippocampal organization but displayed an increase in apoptotic cell death in the developing dentate gyrus; severe deficits on tests of visuospatial learning/memory [104].
Fzd10	Not determined	
Dvl1	*Dvl1*$^{-/-}$; *Dvl2*$^{-/-}$	Skeletal abnormalities and all *Dvl1/2* double mutant embryos displayed craniorachischisis, a completely open neural tube from the midbrain to the tail [105].
Dvl2	*Dvl2*$^{-/-}$	Defects in cardiac neural crest development; ~90% of *Dvl2*$^{-/-}$ mice had vertebral and rib malformations [105].
Dvl3	*Dvl3*$^{-/-}$	Dvl3$^{-/-}$ mice died perinatally due to defects in heart development [106].
Invs (Inv)	*Invs* mutant mice	Inv mutant mice displayed reversed internal organs (situs inversus), multiple renal cysts (polycystic kidney), jaundice and neonatal lethality [107,108].
Vangl1	*Vangl1*$^{gt/+}$ heterozygotes in mice, *Vangl1*$^{gt/+}$ homozygotes in mice	*Vangl1*$^{gt/+}$ heterozygotes and *Vangl1*$^{gt/gt}$ homozygotes were viable and fertile, although *Vangl1*$^{gt/gt}$ had defects in polarity of hair cells of the cochlea [109].
	Vangl1$^{gt/+}$ and *Vangl2*$^{lp/+}$ mice	*Vangl1*$^{gt/+}$; *Vangl2*$^{lp/+}$ double heterozygotes had developmental defects of the brain, inner ear and heart that led to embryonic fatality [109].
Vangl2	Mutation of *Vangl2* (formerly *Lpp1/Ltap*) in the loop-tail mouse	Embryonic fatality due to neural tube defects [92,110–112].
Prickle1	*mpk1*$^{-/-}$ mutant mice (mouse prickle1 also known as mpk1)	Deletion of *mpk1* led to early embryonic lethality at E5.5-E6.5 [113], with mislocalized extracellular matrix (ECM) proteins, and disrupted orientation of mitotic spindles [113].
	Beetlejuice (Bj) mutation in *Prickle1* (Pk1) (Pk1 missense allele called Beetlejuice (Bj))	*Bj* mutants had defects of heart, cochlea and brain development; *Bj* mutants died neonatally with cardiac outflow tract (OFT) malalignment; *Bj* mutant fibroblasts failed to establish polarized cell morphology or engaged in directional cell migration [114].
	Prickle1+/−, *Prickle1*+/*Cys251X*, *Prickle1*+/*Phe141Ser*	Decreased seizure threshold in Pk1 deficient mice [115].
Prickle2	*Prickle2*$^{-/-}$mice, *Prickle2*$^{+/-}$mice.	*Prickle2*$^{-/-}$ mice displayed higher seizure rates than *Prickle2*$^{+/-}$ mice [115].
	Prickle2$^{-/-}$*(Pk2*$^{-/-}$*)*	*Pk2*$^{-/-}$ embryos died at E3.0–3.5 without forming the blastocyst cavity; GTP-bound active form of RhoA was decreased in *Pk2*$^{-/-}$ embryos; defects in apico-basal polarity [116].
Prickle3	*Prickle3*$^{-/-}$	*Prickle3* KO mice had defects in visual development due to degeneration of retinal ganglion cells and abnormal vasculature [117].
Celsr1	Missense mutations within the coding region of Celsr1	Mutation of Celsr1 had PCP defects in hair cells of the cochlea and severe Neural Tube Defects [118].
Celsr2	*Celsr2*-deficient mice	In Celsr2-deficient mice, development and planar organization of ependymal cilia were compromised, leading to defects in CSF dynamics and hydrocephalus [119].
Celsr3	*Celsr3* mutant mice	Defects in brain development with constitutive mutation of *Celsr3* [120,121].
	Celsr2 and *Celsr3* double mutant mice	*Celsr2* and *Celsr3* double mutants led to ependyma, defects in ciliogenesis, resulting in lethal hydrocephalus [119].
	Celsr3$^{-/-}$	Defects in brain development due to failure of axonal projections [121].
Fat1	*Fat1*$^{-/-}$	Perinatal death, defects in brain developmental [122].
	Podocyte-specific deletion of Fat1 in mice	Induces abnormal glomerular filtration barrier development due to defects in podocyte foot process effacement [123].
Fat2	Not determined	Not known
Fat3	Conditional knockout (KO) of *Fat3* in brains of adult mice	Conditional KO of Fat3 in brains of adult mice was obtained using inducible Thy1Cre(ERT2) SLICK H line; behavioral and biochemical analysis revealed that the brain of these had no abnormalities [124].
Fat4	*Fat4*$^{-/-}$, *Dchs1*$^{-/-}$	Dual KO mice had defects in anterior pituitary morphogenesis [125].
	Fat4 knockout mice	*Fat4* KO mice died at birth, defects of hair cell PCP in cochlea, and defects in brain and kidney development [126].
Dchs1	*Dchs1* mutant mouse	Homozygous KO of *Dchs1* in mice led to neonatal lethality and multi-organ impairment [127]; defects in brain development [128].
Dchs2	*Dchs2*$^{-/-}$ mouse mutants	*Dchs2*$^{-/-}$ mutant mice were viable and fertile but with defects in pituitary gland [125].
Fjx1	Null mutation of *Fjx1*	Homozygous *Fjx1* mutants had defects in hippocampus development [129].
	Fjx1$^{-/-}$, *Fat4*$^{-/-}$	Dual deletion of *Fjx1* and *Fat4* led to loss of PCP in the hair cells of cochlea, defects in neural tube, and cyst formation in kidney [130].
	Fjx1, Pkd1 double KO	Survive longer than single *Pkd1* KO mice; reduced fibrogenesis caused by *Fjx1* deletion [130].

mammalian development [3,31,42]. Nonetheless, all the proteins of the Fat/Dchs/Fjx1 pathway have not been studied functionally in the testis, and such investigations are much needed in future studies.

2.1. The PCP Van Gogh-like 2 (Vangl2)/Prickle (Pk) protein complex

2.1.1. Background

The first core PCP protein complex that has been studied in the testis is the Vangl2/Pk complex [15,18]. Mutation of *Vangl1* or *Vangl2* in mice (Table 2), and also mutation of *VANGL1* [43–45] or *VANGL2* [44,46,47] in humans lead to neural-tube defects (Table 3). *Vangl2* knock-out (KO) in mice led to embryonic fatality, which was the result of failure in neural tube development [48–50], as well as defects in lung- [51] and kidney- [52] branching morphogenesis. Interestingly, neural tube defects found in *Vangl1*-mutated mice, however, were less severe compared to *Vangl2* KO mice [50,53]. Vangl2 is a small integral membrane protein of 60 kDa with four transmembrane domains. Studies have shown that Vangl2 is involved in the assembly and stabilization/maintenance of adherens junction (AJ) in the brain and kidney [54–57]. Vangl2 knockdown (KD) by RNAi or through its overexpression in epithelial cell lines HEK293T and MDCK was found to perturb cell-cell and cell-substratum adhesion via changes in cytoskeletal function [58], illustrating the proper level of Vangl2 in cells and tissues are necessary to maintain homeostasis and function of cytoskeletons in cells and tissues.

2.1.2. Vangl2/Pk complex

In the testis, Vangl2 is localized at the Sertoli–Sertoli cell interface but also Sertoli-germ cell interface across the seminiferous epithelium in virtually all stages of the epithelial cycle based on immunofluorescence analysis [15]. Vangl2 appears as track-like structures, similar to the actin- and microtubule (MT)-based cytoskeletons that lay cross the epithelium and align perpendicular to the basement membrane. Vanlg2 partially co-localizes with F-actin and α-tubulin (which together with ß-tubulin create the α-/ß-tubulin oligomers that serve as building blocks of MTs) [15,18]. These findings suggest that Vangl2 may work in concert with actin- and MT-based cytoskeletons to support spermatid PCP during spermatogenesis. Indeed, a knockdown (KD) of Vangl2 by RNAi [15] was found to perturb elongated spermatid PCP wherein the orientation of polarized spermatids that laid across the plane of seminiferous was considerably perturbed [18]. For instance, elongated spermatids no longer aligned correctly but disorganized, and spermatids were also released into the tubule lumen before stage VIII of the epithelial cycle when cellular organization and architecture of seminiferous tubules were dissected and examined by 3D-reconstruction following confocal microscopy [18]. This study thus provides the proof that Vangl2 is indeed a PCP protein in the testis. More important, a KD of Vangl2 by RNAi that reduced the expression of Vangl2 by 70% also altered elongated spermatid adhesion to, and their transport across, the seminiferous epithelium [15]. This conclusion was supported by the observation that many mis-aligned step 19 elongated spermatids with defects in polarity remained embedded across the seminiferous epithelium in stages IX-X tubules [15] when spermiation had occurred at stage VIII of the epithelia cycle. Interestingly, defects of meiosis were also noted in stage XIV tubules when meiosis took place [15]. For instance, there was a 50% reduction in the frequency of meiotic germ cells across the epithelium in cross-sections of tubules in the rat testis following KD of Vangl2 by RNAi vs. testes transfected with non-targeting negative control siRNA duplexes or normal testes [15]. However, it remains to be determined if the reduction in the number of meiotic germ cells noted at stage XIV was due to defects in meiosis, a reduced population of spermatocytes and related to changes in cell adhesion, or both. Nonetheless, Vangl2 KD-induced defects in cytoskeletal organization could be responsible for these changes. Indeed, when the organization of F-actin and MTs across the seminiferous epithelium was examined following Vangl2 KD in the testis in vivo, both cytoskeletons displayed considerable defects. For instance, these cytoskeletons failed to stretch across the seminiferous epithelium as track-like structures, instead they were extensively truncated, and fragments of the F-actin and MTs were also mis-aligned [18]. Unlike the control testes (either normal testes or testes transfected with non-targeting siRNA duplexes) where actin- and MT-based tracks stretched across the entire epithelium and laid perpendicular to the basement membrane [18]. Some fragments of F-actin and MTs were found to be aligned parallel to the basement membrane, making them impossible to serve as tracks to transport cargoes (e.g., residual bodies, phagosomes) and developing spermatids across the seminiferous epithelium. These defects in cytoskeletons thus fail to support meiosis and spermatid PCP since both cellular events require proper organizations of actin and MT cytoskeletons across the epithelium. These findings in vivo are also supported by studies in vitro using primary cultures of Sertoli cells. For instance, in control untreated Sertoli cell epithelium, the linear F-actin and microtubules stretched across the entire cell cytosol, but they were considerably truncated and mis-aligned following Vangl2 knockdown by RNAi [15,18]. Additionally, a study by co-immunoprecipitation (Co-IP) using corresponding specific antibodies has shown that Vangl2 is structurally interacted with Scribble but not other actin regulatory proteins, such as Arp3, Eps8 and also N-cadherin [15]. Scribble is a master scaffolding protein in cell polarity, and also known to confer PCP and cell adhesion [59] through its effects on cytoskeleton [60]. Thus, it is likely that Vangl2 and Scribble may exert their PCP regulating effects as a partner protein pair. This possibility should be carefully evaluated in future studies.

2.1.3. Vangl2 regulates spermatogenesis through signaling proteins PKCζ and MARK2

Studies have shown that Vangl2 exerts its regulatory effects on actin and MT dynamics through changes in the expression of PKCζ (protein kinase C-ζ, a Ser/Thr protein kinase, also an atypical PKC (aPKC) isozyme, known to modulate actin cytoskeletal organization [61,62]) and MARK2 (microtubule affinity-regulating kinase 2, also a Ser/Thr protein kinase and a regulator of MT cytoskeleton [63]) [15,18]. These changes, in turn, modify Sertoli cell function to support spermatid PCP and spermatid adhesion in the seminiferous epithelium. For instance, a KD of Vangl2 in testes in vivo by down-regulating Vangl2 expression by ~70% was found to considerably down-regulate the expression of p-PKCζ-T410 based on immunoblot analysis [18]. This change was accompanied by a disruptive F-actin organization across the seminiferous epithelium [18]. These findings are consistent with an earlier report, illustrating that an imbalanced cellular level of PKCζ is known to perturb the organization of stress fibers across cell cytosol in NIH3T3 cells following overexpression of cDNA constructs encoding constitutively active mutants of PKCζ [62]. Vangl2 KD also downregulated the expression of p-MARK2-T595, which in turn, activated the intrinsic kinase activity of MARK2 [18], thereby promoting structural MAP (microtubule-associated protein, e.g., MAP1a) phosphorylation, causing MAPs detachment from MTs [63]. Since the binding of structural MAPs (e.g., MAP1a) onto MTs promote MT stability, their detachment from MTs following phosphorylation by MARKs (e.g., MARK2) thus promote MT catastrophe (Figs. 3 and 4). These changes thus led to disorganized MT-based tracks across seminiferous epithelium, which appeared as broken and mis-aligned tracks in Vangl2 silenced testes, but also disorganized actin filaments across the epithelium [18] (Figs. 3 and 4). This latter observation was also noted in Vang2 KD Sertoli cells wherein MTs across the Sertoli cell cytosol were grossly truncated, concomitant with a considerable reduction in MT polymerization based on a biochemical assay [18]. These changes in cytoskeletal organization following Vangl2 KD thus perturbed spermatid PCP, which was remarkably noted in 3D reconstructed images by confocal microscopy, and was accompanied by distinctive phenotypes in the testis manifested by extensive spermatid exfoliation from the seminiferous epithelium, possibly as the result of disruptive cytoskeletons [18]. Thus, these findings have unequivocally demonstrated that Vangl2 is a putative PCP

Table 3
Genetic variations and/or mutations of PCP proteins that lead to pathological conditions in humans.

Gene name	Phenotypes
FZD1	Not known
FZD2	Omodysplasia-2 or Robinow syndome-like phenotype [131]; autosomal dominant omodysplasia [132].
FZD3	Hirschsprung disease [133].
FZD4	Familial exudative vitreoretinopathy (FEVR) [134,135].
FZD5	Autosomal dominant non-syndromic coloboma [136].
FZD6	Neural tube defects [137]. Isolated recessive nail dysplasia [138]. Autosomal recessive nail dysplasia [139].
FZD7	Not known
FZD8	Not known
FZD9	Williams-Beuren syndrome with multiple manifestation including low bone mass [140–143].
FZD10	Not known
DVL1	*DVL1* frameshift mutations clustering in the penultimate exon cause autosomal-dominant Robinow syndrome (DRS) [144]; mutations in DVL1 cause an osteosclerotic form of Robinow syndrome (RS-OS) [145].
DVL2	*DVL* mutations, especially *DVL2* p.R633W, may contribute to human neural diseases such as neural tube defects (NTDs) and Dandy-Walker malformation (DWM) by obstructing Wnt signaling pathways [146].
DVL3	*DVL3* alleles resulting in a −1 frameshift of the last exon lead to Autosomal-Dominant Robinow Syndrome [147]; and NTDs [146].
INVS	*INVS* mutations cause nephronophthisis Type 2 [148]; juvenile nephronophthisis with abnormal reactivity of the Wnt/β-catenin pathway [149].
VANGL1	Neural tube defects [45,150].
VANGL2	Defects in cranial neural-tube defects [151]; neural tube defects [46].
PRICKLE1	Homozygous mutation in *PRICKLE1* causes an Autosomal-Recessive Progressive Myoclonus Epilepsy-Ataxia Syndrome [152]; and also autosomal dominant progressive myoclonus epilepsy (due to a single variant in the PRICKLE1 gene) [153].
PRICKLE2	Myoclonic seizures; ataxia; developmental delay; epilepsy; autisic disorder [115].
PRICKLE3	Leber's hereditary optic neuropathy [117].
CELSR1	Hereditary lymphedema [154]; pina bifida [155]; and neural tube defects [156].
CELSR2	Joubert syndrome and growth hormone deficiency [157].
CELSR3	Hirschsprung disease (HSCR) [133]; Tourette disorder [158].
FAT1	Glomerulotubular nephropathy [123]; homozygous frameshift mutations in *FAT1* cause a syndrome characterized by colobomatous-microphthalmia, ptosis, nephropathy and syndactyly [159]; acute lymphoblastic leukemia [160,161]; and facioscapulohumeral dystrophy-like phenotype [162].
FAT2	Spinal meningioma [163]; esophageal squamous cell carcinoma (ESCC) associated with mutated genes such as *FAT1*, *FAT2* [164].
FAT3	External auditory canal squamous cell carcinoma associated with mutated genes such as *FAT1* and *FAT3* [165]; Hirschsprung disease [166].
FAT4	Mutations in the atypical cadherin *FAT4* cause Van Maldergem syndrome, associated with congenital anomalies of the kidney and urinary tract [167,168]; Hennekam syndrome[167]; periventricular neuronal heterotopia [168]; pituitary developmental defects [125].
DCHS1	Mitral valve prolapse[169,170]; *DCHS1* mutations also cause recessive Van Maldergem syndrome, with pleiotropic phenotypes including neuronal periventricular heterotopia [168]; and Myxomatous disease (MMVP2) [171].
DCHS2	Pituitary developmental defects [125]; frameshift mutations of cadherin genes *DCHS2*, *CDH10* and *CDH24* lead to gastric and colorectal cancers [172].
FJX1	Not known

protein in the testis to support spermatid PCP during spermatogenesis through organized cytoskeletons of microtubules and F-actin. This orderly alignment of elongate spermatids during spermiogenesis is necessary to pack the maximal number of developing spermatids across the epithelium to support the production of millions of functional haploid spermatids on a daily basis through the epithelial cycle of spermatogenesis.

Pk1 and Pk2 have been identified in the mouse and human testes [64]. As such, the Vangl2/Pk complex likely maintains spermatid (Fig. 3) and Sertoli cell (Fig. 4) PCP, such as in stage VII tubules, by activating PKCζ (most notably PKCζ-T410), which in turn up-regulates MARK2-T595, rendering MARK2 incapable of phosphorylation structural MAPs (e.g., MAP-1a) [18]. As such, MAP1a binds onto MT to maintain its stability (Figs. 3 and 4). At stage VIII of the epithelial cycle (or when Vangl2 is KD by RNAi [18]), PKCζ-T410 is down-regulated (or inactivated), MARK2 is thus activated, which, in turn, phosphorylates MAPs (e.g., MAP1a), causing their detachment from MTs. As such, MTs are destabilized, undergoing catastrophe (Figs. 3 and 4). F-actin filaments are also disrupted due to disruptive changes in the spatial expression of Arp3 (the branched actin polymerization protein that converts actin filaments from a bundled to a branched configuration, destabilizing apical and basal ES function) and Eps8 (an actin barbed end capping and bundling protein) [15]. These disruptive changes in microtubule and actin cytoskeletons thus contribute to the release of sperm at spermiation and remodeling of the basal ES/BTB to facilitate the transport of preleptotene spermatocytes across the BTB in stage VIII tubules as noted in the hypothetic model shown in Figs. 3 and 4.

2.2. The PCP Frizzled (Fzd)/Dishevelled (Dvl)/Inversin (Invs)/Diversin protein complex

2.2.1. Background

As noted in Fig. 1, the Fzd/Dvl/Inv/diversin is another crucial intercellular complex of the Core Planar Polarity pathway (Table 1). Fzd proteins, namely Fzd1 to 10 (Fig. 2), are transmembrane receptor proteins which interact with the Wnt ligands to induce signaling function [65–67]. FZD3 (FRIZZLED 3) is highly expressed in human testes [68], and FZD9 in mouse testes [69]. Besides the Frizzed receptor protein, there are proteins in the secreted frizzled-related protein (sFRP) family, and at least five secreted proteins have been identified in humans, including sFRP1, sFRP2, sFRP3, sFRP4 and sFRP5. Among these, sFRP1, sFRP2 and sFRP4 have been detected in mouse testes [70,71]. Unlike Fzd, sFRPs are secreted proteins and act as extracellular signaling ligands. However, sFRPs bind to Wnt proteins and Fzd receptors, thereby preventing Wnt proteins from binding to Fzd receptors [72], down-regulating Wnt signaling [73]. Wnt signaling has been shown to be crucial to support embryonic development, cell proliferation and cell

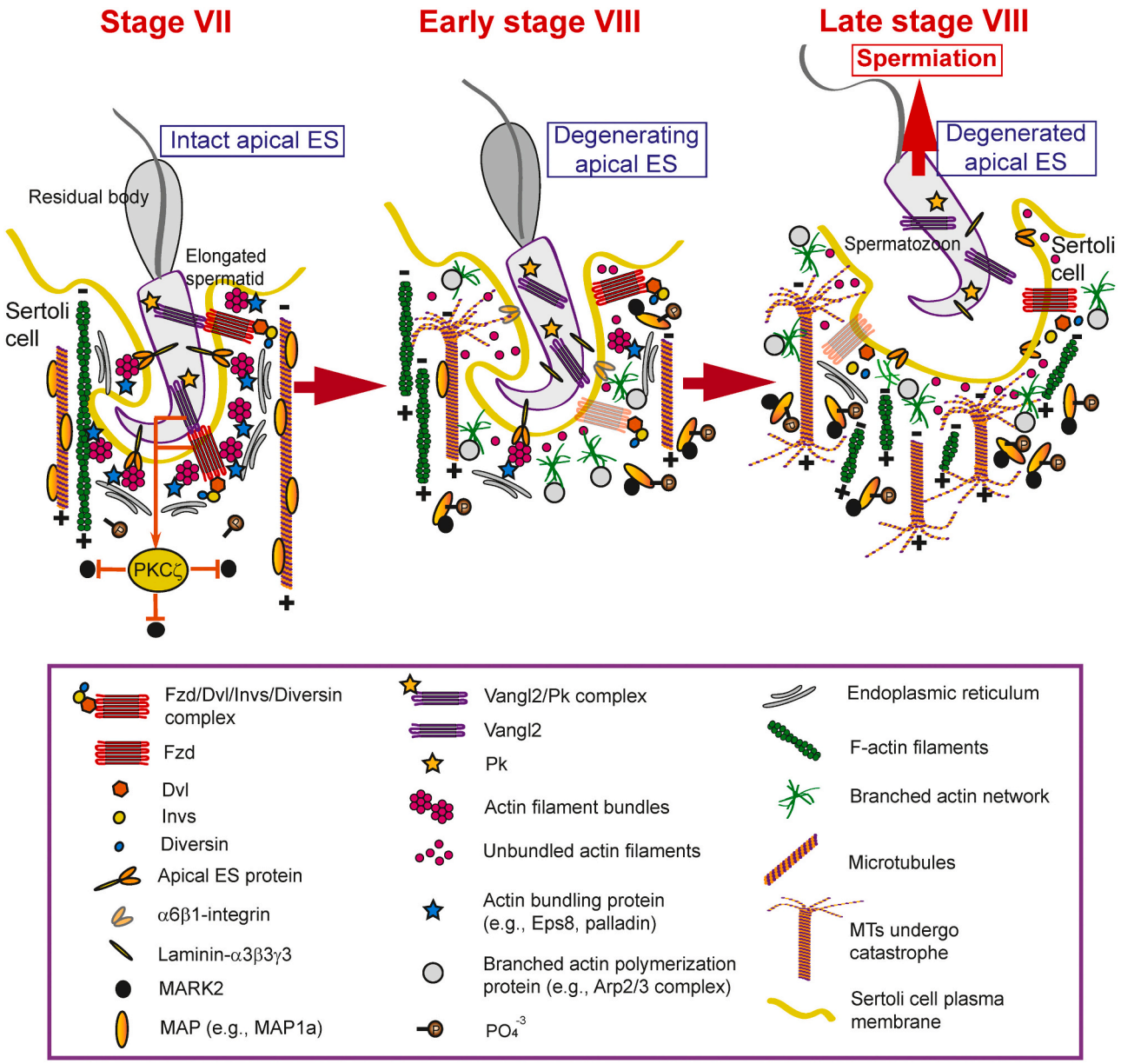

Fig. 3. A hypothetical model on the involvement of Core PCP proteins to support spermatid PCP and sperm release at spermiation through the downstream signaling protein PKCζ. In this model, as noted in the *left* panel of a stage VII tubule, elongated spermatid PCP and spermatid adhesion are maintained by intercellular adhesion bridges of Vangl2/Pk and Fzd/Dvl/inversin/diversin, coupled with the apical ES protein complex of α6ß1-integrin (Sertoli cell) and laminin-α3/ß3/γ3 (elongated spermatid). Integrity of the apical ES is also supported by the actin filament bundles, as well as the adjacent microtubule (MT) and actin cytoskeletons. Furthermore, the Vangl2/Pk complex (and possibly the Fzd/Dvl/Invs/Diversin complex) also promotes (and up-regulates) PKCζ which in turn inactivates MARK2 [18], making MARK2 incapable of phosphorylating structural MAPs (e.g., MAP1a) so that MAPs remain tightly bound to MT filaments to confer MT stability. The Vangl2/Pk complex also promotes F-actin and actin filament bundle stability through its effects on the spatial expression of actin bundling proteins (e.g., palladin, Eps8) to maintain integrity of the actin filament bundles at the apical ES and the actin filaments across the epithelium. At early stage VIII (*middle* panel) through late VIII (*right* panel) of the cycle, a reduction of Vangl2 expression at these stages down-regulates PKCζ, activating MARK2, which in turn, capable of phosphorylateing structural MAPs (e.g., MAP1a) [18], causing detachment of MAPs (e.g., MAP1a) from microtubules. This detachment of structural MAPs from microtubules thus promotes MT catastrophe as noted in the *right* panel, factiliating spermiation, apical ES degeneration, loss of spermatid PCP and also loss of spermatid adhesion. A reduced Vangl2 expression also promotes changes in the spatial expression of branched actin polymerization proteins (e.g., Arp2/3 complex) and down-regulates the expression of Eps8. These changes thus promote unbundling of actin filaments at the apical ES to become a branched network, including F-actin defragmentation [15], to support sperm release at spermiation.

differentiation during development and tumorigenesis, and also cellular homeostasis in cells and tissues during adulthood [65,74–76]. However, the role of Wnt signaling with regard to PCP proteins in the testis remains largely unexplored. It has been reported that sFRP1 is a crucial 37 kDa protein that regulates spermatid adhesion in the testis through its effects on FAK and nectin-3 adhesion protein complex [71]. Based on the available information in the literature, the Fzd/Dvl/Inv complex creates an intercellular complex with Vangl2/Pk to support PCP (Fig. 1; Table 1). More important, the Fzd/Dvl/Inv-Vangl2/Pk intercellular complexes are stabilized by Celsr and/or Fw, but Fzd/Dvl/Inv and Vangl2/Pk are mutually exclusive such that they do not lay adjacent to each other within the same cellular domain (Fig. 1).

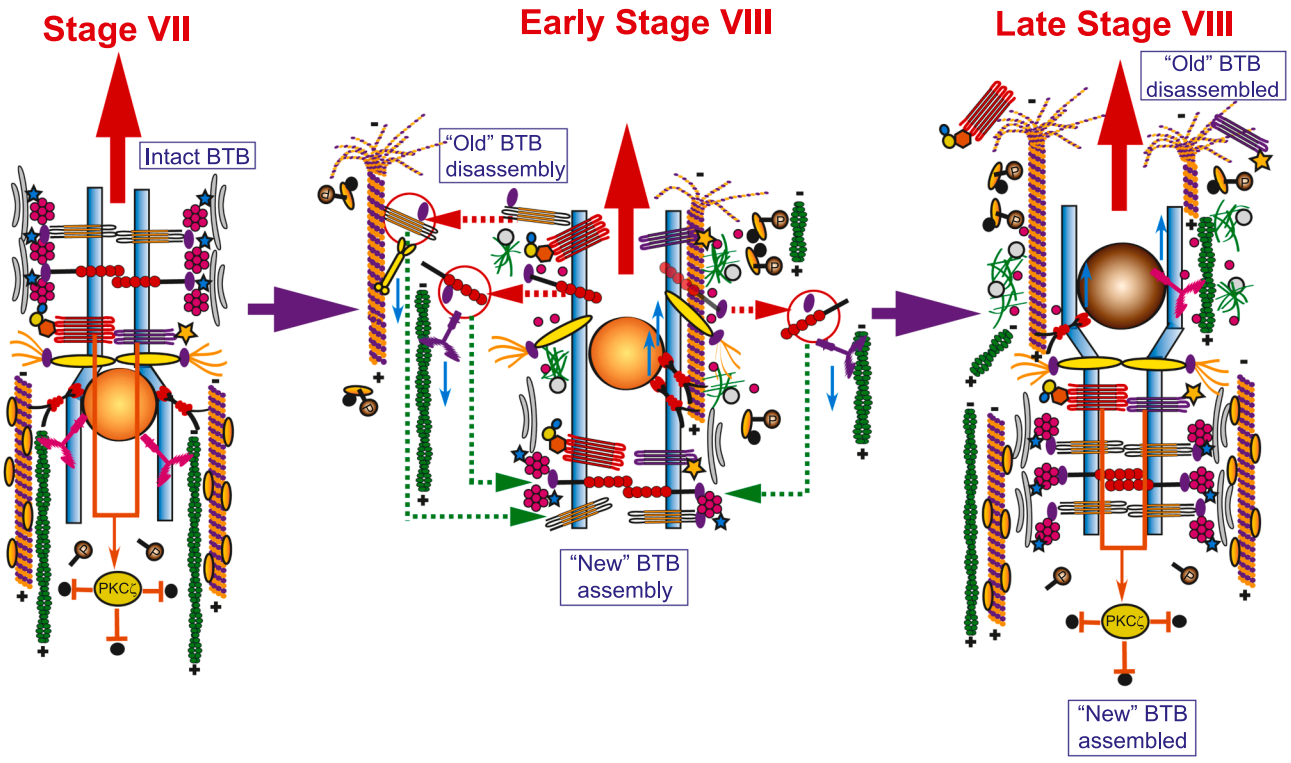

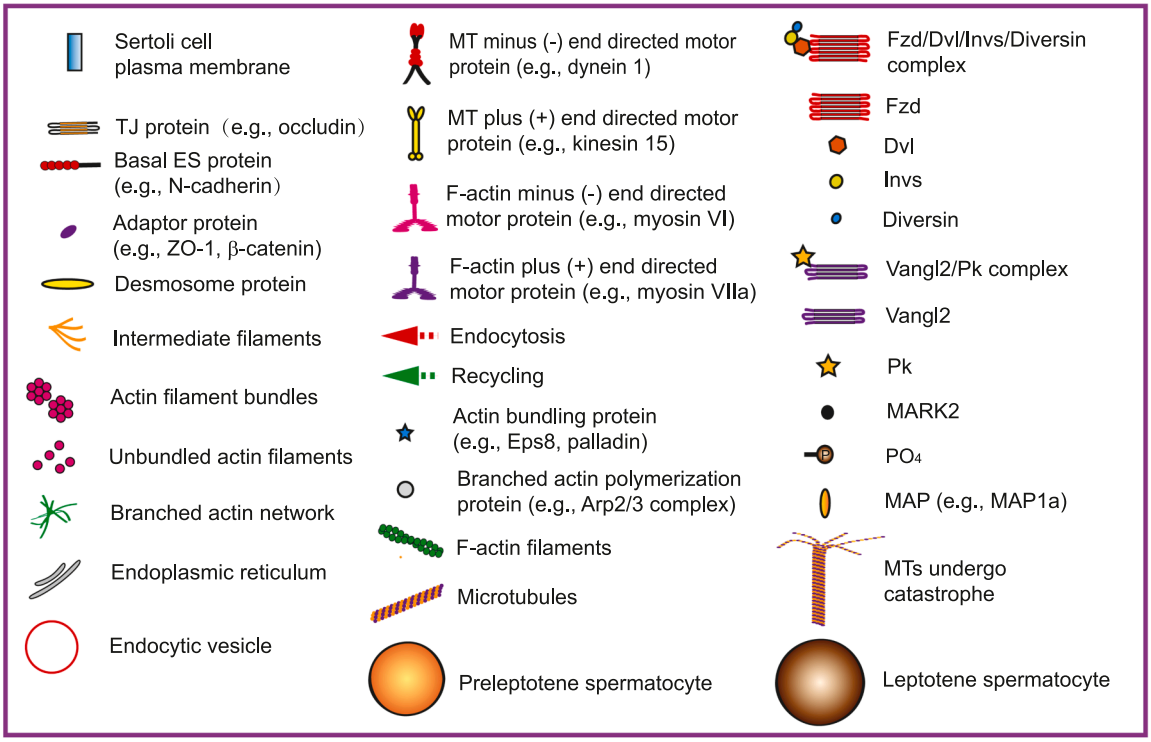

(caption on next page)

Fig. 4. A hypothetical model on the involvement of Core PCP proteins to support BTB remodeling to facilitate the transport of preleptotene spermatocytes across the barrier through the downstream signaling protein PKCζ. In this model, as noted in the *left* panel of a stage VII tubule wherein the BTB is intact. The BTB stability is maintained by the adhesion protein complexes of the actin-based TJ and basal ES, in particular the two arrays of actin filament bundles on both sides of the adjacent Sertoli cells, as well as the intermediate filament-based desmosome. Most importantly, the Vangl2/Pk promotes (and up-regulates) PKCζ which in turn inactivates MARK2 through an up-regulation of p-MARK2-T595, making MARK2 incapable of phosphorylating structural MAPs (e.g., MAP1a) so that MAPs remain tightly bound to MT filaments to confer MT stability. The Vangl2/Pk complex (and most likely Fzd/Dvl complex) also promotes stabilization of the actin filament bundles at the basal ES/BTB, but also F-actin across the seminiferous epithelium. The combined action of these two cytoskeletons across the seminiferous epithelium thus confers BTB/basal ES stability to maintain the BTB integrity. At early stage VIII (*middle* panel) through late VIII (*right* panel) of the cycle, a reduction of Vangl2 expression at these stages thus down-regulates PKCζ, activating MARK2, which in turn, capable of phosphorylating structural MAPs (e.g., MAP1a). This change in turn causes detachment of structural MAPs from microtubules, thereby promoting MT catastrophe as noted in the *middle* panel and *right* panel. At the same time, a reduced Vangl2 expression also promotes spatial expression of branched actin polymerization proteins (e.g., the Arp2/3 complex) to unbundle actin filaments to become a branched network and to promote F-actin defragmentation, thereby destabilizing the actin filament bundles and F-actin network at the site. These changes of the actin- and microtubule cytoskeletons thus promote the transport of preleptotene spermatocytes across the "old BTB" undergoing disassembly. However, a "new" BTB is being assembled behind the spermatocyte due to an increase in Vangl2/Pk complex spatial expression (see *middle* and *right* panels). This in turn up-regulates PKCζ, which inactivates MARK2 [18], promoting the attachment of structural MAPs (e.g., MAP1a) onto microtubules to confer MT stability, and to confer F-actin stabilization [15] to maintain the overall integrity of the basal ES/BTB.

2.2.2. Fzd/Dvl3 complex

While the identity of the Fzd(s) in the testis and the interaction of Fzd with Dvl to create the corresponding Fzd/Dvl intercellular complex(es) remains to be investigated, studies have shown that Dvl 1, Dvl2 and/or Dvl3 are all expressed in rodent testes including the mouse [77,78] and rat [27] testes, but also germ cell tumors in humans [79]. In the mouse testis, Dvl1 displays stage-specific expression [77]. A study by immunohistochemistry (IHC) and fluorescence microscopy have shown that Dvl1 is localized to the cytoplasm of pachytene spermatocytes but also the perinuclear region of developing haploid spermatids, suggesting a role in regulating spermatid morphological transformation during spermiogeneis pertinent to the formation of spermatid head [77]. In the rat testis, Dvl3 is robustly expressed surrounding the entire spermatid heads during spermiogenesis in stage I-V tubules, besides the basal ES at the BTB [27]. However, Dvl3 staining progressively moves away from the perinuclear region of spermatid head, relocating to the tip of spermatid heads until it appears to be engulfed by the Sertoli cell in late stage VII-VIII, but DVl3 continue to express robustly at the basal ES/BTB near the basement membrane [27]. This pattern of stage-specific expression of Dvl3 [27] is similar to results of Dvl1 localization in the mouse testis of an earlier report [77]. Dvl3 also co-localizes with MTs (visualized by α-tubulin staining, which together with ß-tubulin that create the α-/ß-tubulin oligomers, which are the building blocks of MTs), suggesting its possible role in MT dynamics to support spermatogenesis [27]. Studies using genetic models of *Dvl3*$^{-/-}$ mice have shown that deletion of *Dvl3* in mice led to perinatal fatality due to defects in cardiac outflow tract abnormalities [80]. *Dvl3*$^{-/-}$ mice also had defects in the organ of Corti, a structure in the cochlea of the inner ear that produces nerve impulses in response to sound vibrations to support hearing, wherein sterocilia were misorientated due to defects of PCP [80]. *Dvl3* deletion in mice also had defects of transformation of the neural plate into the neural tube, affecting embryonic brain development [80]. Taking collectively, these data indicate that Dvl3 is crucial to mediate PCP signaling to maintain embryonic brain and cochlea development. But the functional significance of Dvl3 in the testis in these earlier reports based on the use of genetic models was not known due to perinatal fatality before these mice could reach maturity.

2.2.3. Studies in vitro

Using RNAi with the corresponding specific siRNA duplexes to knockdown (KD) either Dvl1, Dvl2, Dvl3 or Dvl1/2/3 altogether via triple KD, the role of Dvl1, Dvl2 and Dvl3 on Sertoli cell TJ-permeability barrier function have been examined [27] using primary Sertoli cells cultured in vitro with an established functional TJ-barrier that mimics the BTB in vivo [81]. Dvl3 was found to be crucial to support Sertoli cell BTB function since Dvl3 KD alone was almost as effective as Dvl1/2/3 triple KD to perturb Sertoli cell TJ-permeability barrier function whereas KD of either Dvl1 or Dvl2 alone had a considerable minor effect on Sertoli cell TJ-barrier function [27]. More important, Dvl3 KD profoundly perturbed the organization F-actin and microtubules across the Sertoli cell cytosol [27]. For instance, specific KD of Dvl3 without perturbing the expression of either Dvl1 or Dvl2 in primary Sertoli cells cultured in vitro, F-actin across the Sertoli cell was extensively branched, truncated and mis-aligned [27]. These changes were shown to be mediated through disruptive spatial expression of Arp3 (a branched actin polymerization protein), and accompanied by a considerable reduction in actin polymerization and bundling activity based on biochemical analysis [27]. These changes thus impeded the organization of actin filaments across Sertoli cells to support Sertoli cell TJ-barrier function. On the other hand, Dvl3 specific KD also considerably perturbed microtubule protofilaments since microtubules no longer stretched across the cell cytosol but grossly truncated and retracted to the cell nuclei in Sertoli cells. These changes are possibly mediated by changes in the spatial expression of detryosinated α-tubulin [27] which is known to promote microtubule stabilization [82].

2.2.4. Studies in vivo

The Dvl3 KD mediated defects in Sertoli cell actin- and MT-cytoskeletons following its KD in Sertoli cell epithelium were reproduced in the testis in vivo through the use of a triple KD of Dvl1, Dvl2 and Dvl3 by transfecting testes with the corresponding siRNA duplexes using Polyplus in vivo-jetPEI® transfection reagent with a ~70% efficacy [27]. Following Dvl1/2/3 KD by RNAi, F-actin at the apical ES was considerably dis-organized so that many elongated spermatids had defects in polarity, with groups of elongated spermatids were mis-aligned with their heads no longer pointed toward the basement membrane but were found to tilt away, by at least 90^{o} to 180^{o} from their intended orientation [27]. Also, the MT-based tracks that aligned perpendicular to the basement membrane by stretching across the entire seminiferous epithelium in all stages of the epithelial cycle were extensively truncated, and the remaining defragmented MT-based tracks were considerably mis-aligned. This thus impeded intracellular trafficking of organelles and/or cargoes (e.g.,endocytic vesicles, phagosomes, residual bodies) and the transport of elongated spermatids across the seminiferous epithelium. As such, many multinucleated round spermatids were noted in the seminiferous epithelium [27], due to intracellular trafficking failure to support seminiferous epithelial homeostasis. This conclusion is supported by earlier studies of toxicant- or hormonal disturbance-induced testis injury [83–86] noted in animal models in either rodents, dogs or monkeys. For instance, multinucleated round spermatids and/or spermatocytes were noted across the seminiferous epithelium in these animal models, due to defects in cytoskeletal organization which in turn impeded intracellular trafficking [83,85,87]. Furthermore, Dvl1/2/3 triple KD in the testis in vivo also led to appearance of step 19 spermatids that were embedded deep inside the seminiferous epithelium, co-existing with step 9–12 spermatids in non-stage VIII tubules, such as stages IX, X, XI, and XII tubules [27]. As these step 19 spermatids failed to be transported to the adluminal

compartment near the tubule lumen to undergo spermiation at stage VIII of the epithelial cycle [27]. In brief, these findings thus illustrate the significance of PCP proteins in particular Dvl3 in supporting spermatogenesis, possibly through its involvement in maintaining the homeostasis of actin and MT cytoskeletons.

3. Concluding remarks and future perspectives

We have evaluated recent findings regarding the role of Vangl2 and Dvl3 in Sertoli cells and the testis in supporting spermatogenesis based on recent studies in vitro and in vivo, as Vangl2 and Dvl3 are the crucial components of the PCP Vangl2/Pk and Fzd/Dvl3 intercellular protein complexes of the PCP family (Table 1). Furthermore, recent data, including the signaling proteins (e.g., PKCζ, MARK2) and the signaling cascade downstream of the Vangl2-based PCP complex that support spermatid PCP function in the testis [15,18], have suggested that PCP proteins exert their regulating effects via the actin- and MT-cytoskeletons. Additionally, data from studies of the Fzd/Dvl3-based protein complex that supports PCP in the testis have also shown the involvement of actin and MT cytoskeletons in mediating Dvl3-conferred PCP [27] in the testis. Similar to functional studies of PCP proteins in other epithelia and tissues/organs, it is likely that Vangl2/PK and Fzd/Dvl form an intercellular binding partner to support PCP in spermatids (Fig. 3) and Sertoli cells (Fig. 4) as noted in the hypothetic models. Needless to say, the hypothetical models shown in Figs. 3 and 4 will be updated rapidly when more data are available, but these models will provide a framework to design functional experiments in future studies. These include: identification of the Fzd(s) that create the functional PCP complex with Dvl3 (or Dvl1, Dvl2), inversin and diversin; the Pk (e.g., Pk1 or Pk2) that creates the functional complex with Vangl2; and the signaling proteins and signaling cascade downstream of the Fzd/Dvl/Invs and Vangl2/Pk. Also, the functional significance of Fat/Dchs/Fjx1 PCP complex in the testis will need to be carefully evaluated. More important, the regulatory biomolecule(s) upstream of these PCP protein complexes that work with germ cells and/or Sertoli cells to modulate spermatogenesis will need to be identified. We also provide a summary of the findings in the literature regarding phenotypes detected in rodents following deletion (or mutation) of specific PCP genes (Table 2) Pathological conditions due to mutation (or genetic variation) of PCP genes in humans are noted in Table 3. Table 2 and 3 thus provide the necessary information to investigators who seek to design experiments to explore the role of PCP genes in supporting spermatogenesis using mouse Sertoli cell- or germ cell-specific KO models. Additionally, the use of bioinformatics approach, such as scRNA-Seq transcriptome profiling in rodent and human testes will likely provide many of the missing information, which should be carefully investigated in future studies.

Conflicts of interest

Authors have nothing to declare.

Acknowledgements

This work was supported in part by grants from the National Key Research and Development Program of China (2018YFC1003500 to S. F.), the National Natural Science Foundation of China (NSFC) (81971367 to L.L.), the Wenzhou Science & Technology Bureau (Y20190015 to L.L.), the China Shenzhen Science Technology and Innovative Commission (SZSTI) (SZSTIJCYJ20180508152336419 to C. K.C.W), and the Second Affiliated Hospital & Yuying Children's Hospital of Wenzhou Medical University (to C.Y.C.). L.W. was supported by a China Pharmaceutical University World Explorer Study Abroad Scholarship.

References

[1] M. Montcouquiol, M.W. Kelley, Development and patterning of the cochlea: from convergent extension to planar polarity, Cold Spring Harb. Perspect. Med. 10 (1) (2020), a033266, https://doi.org/10.1101/cshperspect.a033266.
[2] C. Harrison, H. Shao, H. Strutt, D. Strutt, Molecular mechanisms mediating asymmetric subcellular localisation of the core planar polarity pathway proteins, Biochem. Soc. Trans. 48 (4) (2020) 1297–1308.
[3] M.T. Butler, J.B. Wallingford, Planar cell polarity in development and disease, Nat. Rev. Mol. Cell Biol. 18 (6) (2017) 375–388.
[4] H. Chen, D.D. Mruk, W.Y. Lui, C.K.C. Wong, W.M. Lee, C.Y. Cheng, Cell polarity and planar cell polarity (PCP) in spermatogenesis, Semin Cell Dev. Biol. 81 (2018) 71–77.
[5] Y. Yang, M. Mlodzik, Wnt-Frizzled/planar cell polarity signaling: cellular orientation by facing the wind (Wnt), Annu. Rev. Cell Dev. Biol. 31 (2015) 623–646.
[6] L.V. Goodrich, D. Strutt, Principles of planara polarity in animal development, Development 138 (2011) 1877–1892.
[7] E.K. Vladar, D. Antic, J.D. Axelrod, Planar cell polarity signaling: the developing cell's compass, Cold Spring Harb. Perspect. Biol. 1 (2009), a002964.
[8] D. Davenport, The cell biology of planar cell polarity, J. Cell Biol. 207 (2014) 171–179.
[9] J. Cravo, S. van den Heuvel, Tissue polarity and PCP protein function: C. elegans as an emerging model, Curr. Opin. Cell Biol. 62 (2020) 159–167.
[10] R.S. Gray, I. Roszko, L. Solnica-Krezel, Planar cell polarity: coordinating morphogenetic cell behaviors with embryonic polarity, Dev. Cell 21 (2011) 120–133.
[11] J.B. Wallingford, S.E. Fraser, R.M. Harland, Convergent extension: the molecular control of polarized cell movement during embryonic development, Dev. Cell 2 (2002) 695–706.
[12] M. Tada, M. Kai, Planar cell polarity in coordinated and directed movements, Curr. Top. Dev. Biol. 101 (2012) 77–110.
[13] K. VanderVorst, J. Hatakeyama, A. Berg, H. Lee, K.L. Carraway 3rd, Cellular and molecular mechanisms underlying planar cell polarity pathway contributions to cancer malignancy, Semin Cell Dev. Biol. 81 (2018) 78–87.
[14] H. Chen, C.Y. Cheng, Planar cell polarity (PCP) proteins and spermatogenesis, Semin Cell Dev. Biol. 59 (2016) 99–109.
[15] H. Chen, D.D. Mruk, W.M. Lee, C.Y. Cheng, Planar cell polarity (PCP) protein Vangl2 regulates ectoplasmic specialization dynamics via its effects on actin microfilaments in the testes of male rats, Endocrinology 157 (2016) 2140–2159.
[16] Q. Wen, D. Mruk, E.I. Tang, C.K.C. Wong, W.Y. Lui, W.M. Lee, X. Xiao, B. Silvestrini, C.Y. Cheng, Cell polarity and cytoskeletons-Lesson from the testis, Semin Cell Dev. Biol. 81 (2018) 21–32.
[17] L. Hermo, R.M. Pelletier, D.G. Cyr, C.E. Smith, Surfing the wave, cycle, life history, and genes/proteins expressed by testicular germ cells. Part 2: changes in spermatid organelles associated with development of spermatozoa, Microsc. Res Tech. 73 (2010) 279–319.
[18] H. Chen, X. Xiao, W.Y. Lui, W.M. Lee, C.Y. Cheng, Vangl2 regulates spermatid planar cell polarity through microtubule (MT)-based cytoskeleton in the rat testis, Cell Death Dis. 9 (3) (2018) 340.
[19] J.A. Zallen, Planar polarity and tissue morphogenesis, Cell 129 (2007) 1051–1063.
[20] M.-L. Chin, M. Mlodzik, The Drosophila selectin furrowed mediates intercellular planar cell polarity interactions via frizzled stabilization, Dev. Cell 26 (5) (2013) 455–468.
[21] D.D. Tang, B.D. Gerlach, The roles and regulation of the actin cytoskeleton, intermediate filaments and microtubules in smooth muscle cell migration, Respir. Res. 18 (1) (2017) 54.
[22] B.C. Lim, S. Matsumoto, H. Yamamoto, H. Mizuno, J. Kikuta, M. Ishii, A. Kikuchi, Prickle1 promotes focal adhesion disassembly in cooperation with the CLASP-LL5beta complex in migrating cells, J. Cell Sci. 129 (16) (2016) 3115–3129.
[23] Q. Lu, D.A. Schafer, P.N. Adler, The *Drosophila* planar polarity gene multiple wing hairs directly regulates the actin cytoskeleton, Development 142 (2015) 2478–2486.
[24] E. Bailly, A. Walton, J.P. Borg, The planar cell polarity Vangl2 protein: from genetics to cellular and molecular functions, Semin. Cell Dev. Biol. 81 (2018) 62–70.
[25] W.Y. Aw, D. Devenport, Planar cell polarity: global inputs establishing cellular asymmetry, Curr. Opin. Cell Biol. 44 (2017) 110–116.
[26] M. Galic, M. Matis, Polarized trafficking provides spatial cues for planar cell polarization within a tissue, Bioessays 37 (6) (2015) 678–686.
[27] L. Li, B. Mao, M. Yan, S. Wu, R. Ge, Q. Lian, C.Y. Cheng, Planar cell polarity protein Dishevelled 3 (Dvl3) regulates ectoplasmic specialization (ES) dynamics in the testis through changes in cytoskeletal organization, Cell Death Dis. 10 (3) (2019) 194, https://doi.org/10.1038/s41419-019-1394-7).
[28] L. Li, B. Mao, S. Wu, Q. Lian, R.S. Ge, B. Silvestrini, C.Y. Cheng, Regulation of spermatid polarity by the actin- and microtubule (MT)-based cytoskeletons, Semin Cell Dev. Biol. 81 (2018) 88–96.
[29] E.I. Tang, D.D. Mruk, C.Y. Cheng, Regulation of microtubule (MT)-based cytoskeleton in the seminiferous epithelium during spermatogenesis, Semin Cell Dev. Biol. 59 (2016) 35–45.
[30] J.D. Axelrod, Planar cell polarity signaling in the development of left-right asymmetry, Curr. Opin. Cell Biol. 62 (2020) 61–69.
[31] M. Matis, J.D. Axelrod, Regulation of PCP by the Fat signaling pathway, Genes Dev. 27 (20) (2013) 2207–2220.

[32] Y. Keira, M. Wada, H.O. Ishikawa, Regulation of drosophila development by the golgi kinase four-jointed, Curr. Top. Dev. Biol. 123 (2017) 143–179.
[33] S.M. Maung, A. Jenny, Planar cell polarity in *Drosophila*, Organogenesis 7 (2011) 165–179.
[34] M. Mlodzik, Planar cell polarizaation: do the same mechanisms regulate *Drosophila* tissue polarity and vertebrate gastrulation? Trends Genet 18 (2002) 564–571.
[35] M. Mlodzik, The Dishevelled protein family: still rather a mystery after over 20 years of molecular studies, Curr. Top. Dev. Biol. 117 (2016) 75–91.
[36] M. Montcouquiol, N. Sans, D. Huss, J. Kach, J.D. Dickman, A. Forge, R.A. Rachel, N.G. Copeland, N.A. Jenkins, D. Bogani, J. Murdoch, M.E. Warchol, R. J. Wenthold, M.W. Kelley, Asymmetric localization of Vangl2 and Fz3 indicate novel mechanisms for planar cell polarity in mammals, J. Neurosci. 26 (19) (2006) 5265–5275.
[37] D. Devenport, E. Fuchs, Planar polarization in embryonic epidermis orchestrates global asymmetric morphogenesis of hair follicles, Nat. Cell Biol. 10 (11) (2008) 1257–1268.
[38] E. Torban, H.J. Wang, N. Groulx, P. Gros, Independent mutations in mouse Vangl2 that cause neural tube defects in looptail mice impair interaction with members of the Dishevelled family, J. Biol. Chem. 279 (50) (2004) 52703–52713.
[39] A.L. Brittle, A. Repiso, J. Casal, P.A. Lawrence, D. Strutt, Four-jointed modulates growth and planar polarity by reducing the affinity of dachsous for fat, Curr. Biol. 20 (9) (2010) 803–810.
[40] M.A. Simon, A. Xu, H.O. Ishikawa, K.D. Irvine, Modulation of fat:dachsous binding by the cadherin domain kinase four-jointed, Curr. Biol. 20 (9) (2010) 811–817.
[41] R. Hale, A.L. Brittle, K.H. Fisher, N.A. Monk, D. Strutt, Cellular interpretation of the long-range gradient of four-jointed activity in the Drosophila wing, eLife 4 (2015).
[42] Y. Mao, J. Mulvaney, S. Zakaria, T. Yu, K.M. Morgan, S. Allen, M.A. Basson, P. Francis-West, K.D. Irvine, Characterization of a Dchs1 mutant mouse reveals requirements for Dchs1-Fat4 signaling during mammalian development, Development 138 (5) (2011) 947–957.
[43] E. Merello, S. Mascelli, A. Raso, G. Piatelli, A. Consales, A. Cama, Z. Kibar, V. Capra, P.D. Marco, Expanding the mutational spectrum associated to neural tube defects: literature revision and description of novel VANGL1 mutations, Birth Defects Res. A Clin. Mol. Teratol. 103 (2015) 51–61.
[44] A. Iliescu, M. Gravel, C. Horth, P. Gros, Independent mutations at Arg181 and Arg274 of Vangl proteins that are associated with neural tube defects in humans decrease protein stability and impair membrane targeting, Biochemistry 53 (32) (2014) 5356–5364.
[45] Z. Kibar, E. Torban, J.R. McDearmid, A. Reynolds, J. Berghout, M. Mathieu, I. Kirillova, P. De Marco, E. Merello, J.M. Hayes, J.B. Wallingford, P. Drapeau, V. Capra, P. Gros, Mutations in VANGL1 associated with neural-tube defects, New Engl. J. Med. 356 (14) (2007) 1432–1437.
[46] Z. Kibar, S. Salem, C.M. Bosoi, E. Pauwels, P. De Marco, E. Merello, A.G. Bassuk, V. Capra, P. Gros, Contribution of VANGL2 mutations to isolated neural tube defects, Clin. Genet. 80 (1) (2011) 76–82.
[47] Y.P. Lei, T. Zhang, H. Li, B.L. Wu, L. Jin, H.Y. Wang, VANGL2 mutations in human cranial neural-tube defects, N. Engl. J. Med 362 (2232–2235) (2010).
[48] H. Yin, C.O. Copley, L.V. Goodrich, M.R. Deans, Comparison of phenotypes between different vangl2 mutants demonstrates dominant effects of the Looptail mutation during hair cell development, PLoS One 7 (2) (2012), e31988.
[49] Z. Kibar, K.J. Vogan, N. Groulx, M.J. Justice, D.A. Underhill, P. Gros, Ltap, a mammalian homolog of *Drosophila* Strabismus/Van Gogh, is altered in the mouse neural tube mutant Loop-tail, Nat. Genet. 28 (2001) 251–255.
[50] E. Torban, A.M. Patenaude, S. Leclerc, S. Rakowiecki, S. Gauthier, G. Andelfinger, D.J. Epstein, P. Gros, Genetic interaction between members of the Vangl family causes neural tube defects in mice, Proc. Natl. Acad. Sci. U.S.A. 105 (2008) 3449–3454.
[51] L.L. Yates, C. Schnatwinkel, J.N. Murdoch, D. Bogani, C.J. Formstone, S. Townsend, A. Greenfield, L.A. Niswander, C.H. Dean, The PCP genes Celsr1 and Vangl2 are required for normal lung branching morphogenesis, Hum. Mol. Genet. 19 (2010) 2251–2267.
[52] L.L. Yates, J. Papakrivopoulou, D.A. Long, P. Goggolidou, J.O. Connolly, A. S. Woolf, C.H. Dean, The planar cell polarity gene Vangl2 is required for mammalian kidney-branching morphogenesis and glomerular maturation, Hum. Mol. Genet. 19 (2010) 4663–4676.
[53] H. Song, H. Jianxin, W. Chen, G. Elliott, P. Andre, B. Gao, Y. Yang, Planar cell polarity breaks bilateral symmetry by controlling ciliary positioning, Nature 466 (2010) 378–383.
[54] B.L. Rocque, S. Babayeva, J. Li, V. Leung, L. Nezvitsky, A.V. Cybulsky, P. Gros, E. Torban, Deficiency of the planar cell polarity protein Vangl2 in podocytes affects glomerular morphogenesis and increases susceptibility to injury, J. Am. Soc. Nephrol. 26 (2015) 576–586.
[55] T. Nagaoka, R. Ohashi, A. Inutsuka, S. Sakai, N. Fujisawa, M. Yokoyama, Y. H. Huang, M. Igarashi, M. Kishi, The Wnt/planar cell polarity pathway component Vangl2 induces synapse formation through direct control of N-cadherin, Cell Rep. 6 (5) (2014) 916–927.
[56] T. Nagaoka, A. Inutsuka, K. Begum, K. Bin hafiz, M. Kishi, Vangl2 regulates E-cadherin in epithelial cells, Sci. Rep. 4 (2014) 6940.
[57] E. Torban, A. Iliescu, P. Gros, An expanding role of Vangl proteins in embryonic development, Curr. Top. Dev. Biol. 101 (2012) 237–261.
[58] M. Lindqvist, Z. Horn, v Bryja, G. Schulte, P. Papachristou, R. Ajima, C. Dyberg, A. E, T.P. Yamaguchi, H. Lagercrantz, T. Ringstedt, Vang-like protein 2and Rac1 interact to regulate adherens junctions, J. Cell Sci. 123 (2010) 472–483.
[59] T.T. Bonello, M. Peifer, Scribble: a master scaffold in polarity, adhesion, synaptogenesis, and proliferation, J. Cell Biol. 218 (3) (2019) 742–756.
[60] W.H. Su, E.W.P. Wong, D.D. Mruk, C.Y. Cheng, The Scribble/Lgl/Dlg polarity protein complex is a regulator of blood-testis barrier dynamics and spermatid polarity during spermatogenesis, Endocrinology 153 (2012) 6041–6053.
[61] K. Hellbert, S. Kampfer, K. Maly, F. Hochholdinger, J. Mwanjewe, G. Baier, F. Uberall, H.H. Grunicke, Implication of atypical protein kinase C isozymes lambda and zeta in Ras mediated reorganization of the actin cytoskeleton and cyclin D1-induction, Adv. Enzym. Regul. 40 (2000) 49–62.
[62] F. Uberall, K. Hellbert, S. Kampfer, K. Maly, A. Villunger, M. Spitaler, J. Mwanjewe, G. Baier-Bitterlich, G. Baier, H.H. Grunicke, Evidence that atypical protein kinase C-lambda and atypical protein kinase C-zeta participate in Ras-mediated reorganization of the F-actin cytoskeleton, J. Cell Biol. 144 (3) (1999) 413–425.
[63] A. Ramkumar, B.Y. Jong, K.M. Ori-McKenney, ReMAPping the microtubule landscape: How phosphorylation dictates the activities of microtubule-associated proteins, Dev. Dyn. 247 (2018) 138–155.
[64] M. Katoh, M. Katoh, Identification and characterization of human PRICKLE1 and PRICKLE2 genes as well as mouse Prickle1 and Prickle2 genes homologous to Drosophila tissue polarity gene prickle, Int. J. Mol. Med. 11 (2) (2003) 249–256.
[65] K. Baumann, Switching off WNT with precision, Nat. Rev. Mol. Cell Biol. 16 (4) (2015) 204–205.
[66] G.M. Collu, A. Hidalgo-Sastre, K. Brennan, Wnt-Notch signalling crosstalk in development and disease, Cell Mol. Life Sci. 71 (18) (2014) 3553–3567.
[67] K.W. Pond, K. Doubrovinski, C.A. Thorne, Wnt/β-catenin signaling in tissue self-organization, Genes 11 (8) (2020) 939.
[68] Y.K. Wang, C.H. Samos, R. Peoples, L.A. Pérez-Jurado, R. Nusse, U. Francke, A novel human homologue of the Drosophila frizzled wnt receptor gene binds wingless protein and is in the Williams syndrome deletion at 7q11.23, Hum. Mol. Genet. 6 (3) (1997) 465–472.
[69] Y.K. Wang, R. Spörle, T. Paperna, K. Schughart, U. Francke, Characterization and expression pattern of the frizzled gene Fzd9, the mouse homolog of FZD9 which is deleted in Williams-Beuren syndrome, Genomics 57 (2) (1999) 235–248.
[70] C. Leimeister, A. Bach, M. Gessler, Developmental expression patterns of mouse sFRP genes encoding members of the secreted frizzled related protein family, Mech. Dev. 75 (1–2) (1998) 29–42.
[71] E.W.P. Wong, W.M. Lee, C.Y. Cheng, Secreted Frizzled-related protein 1 (sFRP1) regulates spermatid adhesion in the testis via dephosphorylation of focal adhesion kinase and the nectin-3 adhesion protein complex, FASEB J. 27 (2013) 464–477.
[72] J. Veeck, D. Niederacher, H. An, E. Klopocki, F. Wiesmann, B. Betz, O. Galm, O. Camara, M. Dürst, G. Kristiansen, C. Huszka, R. Knüchel, E. Dahl, Aberrant methylation of the Wnt antagonist SFRP1 in breast cancer is associated with unfavourable prognosis, Oncogene 25 (24) (2006) 3479–3488.
[73] C.S. Chim, R. Pang, T.K. Fung, C.L. Choi, R. Liang, Epigenetic dysregulation of Wnt signaling pathway in multiple myeloma, Leukemia 21 (12) (2007) 2527–2536.
[74] J. Bian, M. Dannappel, C. Wan, R. Firestein, Transcriptional regulation of Wnt/β-catenin pathway in colorectal cancer, Cells 9 (9) (2020) 2125.
[75] M.J. Perugorria, P. Olaizola, I. Labiano, A. Esparza-Baquer, M. Marzioni, J.J. G. Marin, L. Bujanda, J.M. Banales, Wnt-β-catenin signalling in liver development, health and disease, Nat. Rev. Gastroenterol. Hepatol. 16 (2) (2019) 121–136.
[76] C. Siebel, U. Lendahl, Notch signaling in development, tissue homeostasis, and disease, Physiol. Rev. 97 (4) (2017) 1235–1294.
[77] P. Ma, H. Wang, R. Guo, Q. Ma, Z. Yu, Y. Jiang, Y. Ge, J. Ma, S. Xue, D. Han, Stage-dependent Dishevelled-1 expression during mouse spermatogenesis suggests a role in regulating spermatid morphological changes, Mol. Reprod. Dev. 73 (6) (2006) 774–783.
[78] D.J. Sussman, J. Klingensmith, P. Salinas, P.S. Adams, R. Nusse, N. Perrimon, Isolation and characterization of a mouse homolog of the Drosophila segment polarity gene Dishevelled, Dev. Biol. 166 (1) (1994) 73–86.
[79] D. Fabijanovic, I. Zunic, T.N. Martic, F. Skenderi, L. Serman, S. Vranic, The expression of SFRP1, SFRP3, DVL1, and DVL2 proteins in testicular germ cell tumors, Acta Pathol. Microbiol Immunol. Scand. 124 (11) (2016) 942–949.
[80] S.L. Etheridge, S. Ray, S.D. Li, N.S. Hamblet, N. Lijam, M. Tsang, J. Greer, N. Kardos, J.B. Wang, D.J. Sussman, P. Chen, A. Wynshaw-Boris, Murine Dishevelled 3 functions in redundant pathways with Dishevelled 1 and 2 in normal cardiac outflow tract, cochlea, and neural tube development, PLoS Genet 4 (e1000259) (2008), e1000259, https://doi.org/10.1371/journal.pgen.1000259.
[81] D.D. Mruk, C.Y. Cheng, An in vitro system to study Sertoli cell blood-testis barrier dynamics, Methods Mol. Biol. 763 (2011) 237–252.
[82] C. Janke, The tubulin code: molecular components, readout mechanisms, and functions, J. Cell Biol. 206 (4) (2014) 461–472.
[83] K.J. Johnson, Testicular histopathology associated with disruption of the Sertoli cell cytoskeleton, Spermatogenesis 4 (2014), e979106, https://doi.org/10.4161/21565562.2014.979106.
[84] J.D. Vidal, K.M. Whitney, Morphologic manifestations of testicular and epididymal toxicity, Spermatogenesis 4 (2) (2014), e979099.
[85] L. O'Donnell, Mechanisms of spermiogenesis and spermiation and how they are disturbed, Spermatogenesis 4 (2) (2014), e979623.
[86] C.Y. Cheng, Toxicants target cell junctions in the testis: Insights from the indazole-carboxylic acid model, Spermatogenesis 4 (2014), e981485, https://doi.org/10.4161/21565562.2014.9814895.
[87] K. Boekelheide, M.D. Neely, T.M. Sioussat, The Sertoli cell cytoskeleton: a target for toxicant-induced germ cell loss, Toxicol. Appl. Pharm. 101 (1989) 373–389.

[88] H. Matakatsu, S.S. Blair, Interactions between Fat and Dachsous and the regulation of planar cell polarity in the Drosophila wing, Development 131 (15) (2004) 3785–3794.
[89] A.A. Ambegaonkar, G. Pan, M. Mani, Y. Feng, K.D. Irvine, Propagation of Dachsous-Fat planar cell polarity, Curr. Biol. 22 (14) (2012) 1302–1308.
[90] F. Bosveld, I. Bonnet, B. Guirao, S. Tlili, Z. Wang, A. Petitalot, R. Marchand, P. L. Bardet, P. Marcq, F. Graner, Y. Bellaïche, Mechanical control of morphogenesis by Fat/Dachsous/Four-jointed planar cell polarity pathway, Science 336 (6082) (2012) 724–727.
[91] H.O. Ishikawa, H. Takeuchi, R.S. Haltiwanger, K.D. Irvine, Four-jointed is a Golgi kinase that phosphorylates a subset of cadherin domains, Science 321 (5887) (2008) 401–404.
[92] H. Yu, P.M. Smallwood, Y. Wang, R. Vidaltamayo, R. Reed, J. Nathans, Frizzled 1 and frizzled 2 genes function in palate, ventricular septum and neural tube closure: general implications for tissue fusion processes, Development 137 (21) (2010) 3707–3717.
[93] Y. Wang, N. Thekdi, P.M. Smallwood, J.P. Macke, J. Nathans, Frizzled-3Is required for the development of major fiber tracts in the rostral CNS, J. Neurosci. 22 (19) (2002) 8563–8573.
[94] A.I. Lyuksyutova, C.-C. Lu, N. Milanesio, L.A. King, N. Guo, Y. Wang, J. Nathans, M. Tessier-Lavigne, Y. Zou, Anterior-posterior guidance of commissural axons by Wnt-frizzled signaling, Science 302 (5652) (2003) 1984–1988.
[95] Y. Wang, N. Guo, J. Nathans, The role of Frizzled3 and Frizzled6 in neural tube closure and in the planar polarity of inner-ear sensory hair cells, J. Neurosci. 26 (8) (2006) 2147–2156.
[96] Y. Wang, D. Huso, H. Cahill, D. Ryugo, J. Nathans, Progressive cerebellar, auditory, and esophageal dysfunction caused by targeted disruption of the frizzled-4 gene, J. Neurosci. 21 (13) (2001) 4761–4771.
[97] Q. Xu, Y. Wang, A. Dabdoub, P.M. Smallwood, J. Williams, C. Woods, M. W. Kelley, L. Jiang, W. Tasman, K. Zhang, J. Nathans, Vascular development in the retina and inner ear, Cell 116 (6) (2004) 883–895.
[98] T. Ishikawa, Y. Tamai, A.M. Zorn, H. Yoshida, M.F. Seldin, S. Nishikawa, M. M. Taketo, Mouse Wnt receptor gene Fzd5 is essential for yolk sac and placental angiogenesis, Development 128 (1) (2001) 25–33.
[99] N. Guo, C. Hawkins, J. Nathans, Frizzled6 controls hair patterning in mice, Proc. Natl. Acad. Sci. U.S.A. 101 (25) (2004) 9277–9281.
[100] H. Yu, X. Ye, N. Guo, J. Nathans, Frizzled 2 and frizzled 7 function redundantly in convergent extension and closure of the ventricular septum and palate: evidence for a network of interacting genes, Development 139 (23) (2012) 4383–4394.
[101] J. Albers, J. Keller, A. Baranowsky, F.T. Beil, P. Catala-Lehnen, J. Schulze, M. Amling, T. Schinke, Canonical Wnt signaling inhibits osteoclastogenesis independent of osteoprotegerin, J. Cell Biol. 200 (4) (2013) 537–549.
[102] J. Albers, J. Schulze, F.T. Beil, M. Gebauer, A. Baranowsky, J. Keller, R. P. Marshall, K. Wintges, F.W. Friedrich, M. Priemel, A.F. Schilling, J.M. Rueger, K. Cornils, B. Fehse, T. Streichert, G. Sauter, F. Jakob, K.L. Insogna, B. Pober, K. P. Knobeloch, U. Francke, M. Amling, T. Schinke, Control of bone formation by the serpentine receptor Frizzled-9, J. Cell Biol. 192 (6) (2011) 1057–1072.
[103] E.A. Ranheim, H.C. Kwan, T. Reya, Y.K. Wang, I.L. Weissman, U. Francke, Frizzled 9 knock-out mice have abnormal B-cell development, Blood 105 (6) (2005) 2487–2494.
[104] C. Zhao, C. Aviles, R.A. Abel, C.R. Almli, P. McQuillen, S.J. Pleasure, Hippocampal and visuospatial learning defects in mice with a deletion of frizzled 9, a gene in the Williams syndrome deletion interval, Development 132 (12) (2005) 2917–2927.
[105] N.S. Hamblet, N. Lijam, P. Ruiz-Lozano, J. Wang, Y. Yang, Z. Luo, L. Mei, K. R. Chien, D.J. Sussman, A. Wynshaw-Boris, Dishevelled 2 is essential for cardiac outflow tract development, somite segmentation and neural tube closure, Development 129 (24) (2002) 5827–5838.
[106] S.L. Etheridge, S. Ray, S. Li, N.S. Hamblet, N. Lijam, M. Tsang, J. Greer, N. Kardos, J. Wang, D.J. Sussman, P. Chen, A. Wynshaw-Boris, Murine dishevelled 3 functions in redundant pathways with dishevelled 1 and 2 in normal cardiac outflow tract, cochlea, and neural tube development, PLoS Genet. 4 (11) (2008), e1000259.
[107] T. Mochizuki, Y. Saijoh, K. Tsuchiya, Y. Shirayoshi, S. Takai, C. Taya, H. Yonekawa, K. Yamada, H. Nihei, N. Nakatsuji, P.A. Overbeek, H. Hamada, T. Yokoyama, Cloning of inv, a gene that controls left/right asymmetry and kidney development, Nature 395 (6698) (1998) 177–181.
[108] D. Morgan, L. Turnpenny, J. Goodship, W. Dai, K. Majumder, L. Matthews, A. Gardner, G. Schuster, L. Vien, W. Harrison, F.F. Elder, M. Penman-Splitt, P. Overbeek, T. Strachan, Inversin, a novel gene in the vertebrate left-right axis pathway, is partially deleted in the inv mouse, Nat. Genet. 20 (2) (1998) 149–156.
[109] E. Torban, A.M. Patenaude, S. Leclerc, S. Rakowiecki, S. Gauthier, G. Andelfinger, D.J. Epstein, P. Gros, Genetic interaction between members of the Vangl family causes neural tube defects in mice, Proc. Natl. Acad. Sci. U.S.A. 105 (9) (2008) 3449–3454.
[110] Z. Kibar, K.J. Vogan, N. Groulx, M.J. Justice, D.A. Underhill, P. Gros, Ltap, a mammalian homolog of Drosophila Strabismus/Van Gogh, is altered in the mouse neural tube mutant Loop-tail, Nat. Genet. 28 (3) (2001) 251–255.
[111] J.N. Murdoch, K. Doudney, C. Paternotte, A.J. Copp, P. Stanier, Severe neural tube defects in the loop-tail mouse result from mutation of Lpp1, a novel gene involved in floor plate specification, Hum. Mol. Genet. 10 (22) (2001) 2593–2601.
[112] M. Montcouquiol, R.A. Rachel, P.J. Lanford, N.G. Copeland, N.A. Jenkins, M. W. Kelley, Identification of Vangl2 and Scrb1 as planar polarity genes in mammals, Nature 423 (6936) (2003) 173–177.
[113] H. Tao, M. Suzuk, H. Kiyonari, T. Abe, T. Sasaok, N. Ueno, Mouse prickle1, the homolog of a PCP gene, is essential for epiblast apical-basal polarity, Proc. Natl. Acad. Sci. U.S.A. 106 (34) (2009) 14426–14431.
[114] B.C. Gibbs, R.R. Damerla, E.K. Vladar, B. Chatterjee, Y. Wan, X. Liu, C. Cui, G. C. Gabriel, M. Zahid, H. Yagi, H.L. Szabo-Rogers, K.L. Suyama, J.D. Axelrod, C. W. Lo, Prickle1 mutation causes planar cell polarity and directional cell migration defects associated with cardiac outflow tract anomalies and other structural birth defects, Biol. Open 5 (3) (2016) 323–335.
[115] H. Tao, J.R. Manak, L. Sowers, X. Mei, H. Kiyonari, T. Abe, N.S. Dahdaleh, T. Yang, S. Wu, S. Chen, M.H. Fox, C. Gurnett, T. Montine, T. Bird, L.G. Shaffer, J. A. Rosenfeld, J. McConnell, S. Madan-Khetarpal, E. Berry-Kravis, H. Griesbach, R. P. Saneto, M.P. Scott, D. Antic, J. Reed, R. Boland, S.N. Ehaideb, H. El-Shanti, V. B. Mahajan, P.J. Ferguson, J.D. Axelrod, A.E. Lehesjoki, B. Fritzsch, D. C. Slusarski, J. Wemmie, N. Ueno, A.G. Bassuk, Mutations in prickle orthologs cause seizures in flies, mice, and humans, Am. J. Hum. Genet. 88 (2) (2011) 138–149.
[116] H. Tao, K. Inoue, H. Kiyonari, A.G. Bassuk, J.D. Axelrod, H. Sasaki, S. Aizawa, N. Ueno, Nuclear localization of Prickle2 is required to establish cell polarity during early mouse embryogenesis, Dev. Biol. 364 (2) (2012) 138–148.
[117] J. Yu, X. Liang, Y. Ji, C. Ai, J. Liu, L. Zhu, Z. Nie, X. Jin, C. Wang, J. Zhang, F. Zhao, S. Mei, X. Zhao, X. Zhou, M. Zhang, M. Wang, T. Huang, P. Jiang, M. X. Guan, PRICKLE3 linked to ATPase biogenesis manifested Leber's hereditary optic neuropathy, J. Clin. Invest. 130 (9) (2020) 4935–4946.
[118] J.A. Curtin, E. Quint, V. Tsipouri, R.M. Arkell, B. Cattanach, A.J. Copp, D. J. Henderson, N. Spurr, P. Stanier, E.M. Fisher, P.M. Nolan, K.P. Steel, S.D. M. Brown, I.C. Gray, J.N. Murdoch, Mutation of Celsr1 disrupts planar polarity of inner ear hair cells and causes severe neural tube defects in the mouse, Curr. Biol. 13 (13) (2003) 1129–1133.
[119] F. Tissir, Y. Qu, M. Montcouquiol, L. Zhou, K. Komatsu, D. Shi, T. Fujimori, J. Labeau, D. Tyteca, P. Courtoy, Y. Poumay, T. Uemura, A.M. Goffinet, Lack of cadherins Celsr2 and Celsr3 impairs ependymal ciliogenesis, leading to fatal hydrocephalus, Nat. Neurosci. 13 (6) (2010) 700–707.
[120] L. Zhou, Y. Qu, F. Tissir, A.M. Goffinet, Role of the atypical cadherin Celsr3 during development of the internal capsule, Cereb. Cortex 19 (Suppl 1) (2009) i114–i119.
[121] J. Feng, Q. Han, L. Zhou, Planar cell polarity genes, Celsr1-3, in neural development, Neurosci. Bull. 28 (3) (2012) 309–315.
[122] L. Ciani, A. Patel, N.D. Allen, C. ffrench-Constant, Mice lacking the giant protocadherin mFAT1 exhibit renal slit junction abnormalities and a partially penetrant cyclopia and anophthalmia phenotype, Mol. Cell Biol. 23 (10) (2003) 3575–3582.
[123] H.Y. Gee, C.E. Sadowski, P.K. Aggarwal, J.D. Porath, T.A. Yakulov, M. Schueler, S. Lovric, S. Ashraf, D.A. Braun, J. Halbritter, H. Fang, R. Airik, V. Vega-Warner, K.J. Cho, T.A. Chan, L.G. Morris, C. ffrench-Constant, N. Allen, H. McNeill, R. Buscher, H. Kyrieleis, M. Wallot, A. Gaspert, T. Kistler, D.V. Milford, M. A. Saleem, W.T. Keng, S.I. Alexander, R.P. Valentini, C. Licht, J.C. Teh, R. Bogdanovic, A. Koziell, A. Bierzynska, N.A. Soliman, E.A. Otto, R.P. Lifton, L. B. Holzman, N.E. Sibinga, G. Walz, A. Tufro, F. Hildebrandt, FAT1 mutations cause a glomerulotubular nephropathy, Nat. Commun. 7 (2016) 10822.
[124] O. Baron, D. Grieshober, C. Dias, M. Fanto, Fat cadherins in mouse models of degenerative ataxias, Sci. Rep. 9 (1) (2019) 16155.
[125] E.J. Lodge, P. Xekouki, T.S. Silva, C. Kochi, C.A. Longui, F.R. Faucz, A. Santambrogio, J.L. Mills, N. Pankratz, J. Lane, D. Sosnowska, T. Hodgson, A. L. Patist, P. Francis-West, F. Helmbacher, C. Stratakis, C.L. Andoniadou, Requirement of FAT and DCHS protocadherins during hypothalamic-pituitary development, JCI Insight 5 (23) (2020).
[126] S. Saburi, I. Hester, E. Fischer, M. Pontoglio, V. Eremina, M. Gessler, S.E. Quaggin, R. Harrison, R. Mount, H. McNeill, Loss of Fat4 disrupts PCP signaling and oriented cell division and leads to cystic kidney disease, Nat. Genet. 40 (8) (2008) 1010–1015.
[127] Y. Mao, J. Mulvaney, S. Zakaria, T. Yu, K.M. Morgan, S. Allen, M.A. Basson, P. Francis-West, K.D. Irvine, Characterization of a Dchs1 mutant mouse reveals requirements for Dchs1-Fat4 signaling during mammalian development, Development 138 (5) (2011) 947–957.
[128] S. Zakaria, Y. Mao, A. Kuta, C.F. de Sousa, G.O. Gaufo, H. McNeill, R. Hindges, S. Guthrie, K.D. Irvine, P.H. Francis-West, Regulation of neuronal migration by Dchs1-Fat4 planar cell polarity, Curr. Biol. 24 (14) (2014) 1620–1627.
[129] B. Probst, R. Rock, M. Gessler, A. Vortkamp, A.W. Püschel, The rodent Four-jointed ortholog Fjx1 regulates dendrite extension, Dev. Biol. 312 (1) (2007) 461–470.
[130] C. Formica, H. Happe, K.A. Veraar, A. Vortkamp, M. Scharpfenecker, H. McNeill, D.J. Peters, Four-jointed knock-out delays renal failure in an ADPKD model with kidney injury, J. Pathol. 249 (1) (2019) 114–125.
[131] K. Nagasaki, G. Nishimura, T. Kikuchi, H. Nyuzuki, S. Sasaki, Y. Ogawa, A. Saitoh, Nonsense mutations in FZD2 cause autosomal-dominant omodysplasia: Robinow syndrome-like phenotypes, AM J. Med. Genet. Part A 176 (3) (2018) 739–742.
[132] H.M. Saal, C.A. Prows, I. Guerreiro, M. Donlin, L. Knudson, K.L. Sund, C.F. Chang, S.A. Brugmann, R.W. Stottmann, A mutation in FRIZZLED2 impairs Wnt signaling and causes autosomal dominant omodysplasia, Hum. Mol. Genet. 24 (12) (2015) 3399–3409.
[133] L. Su, Z. Zhang, L. Gan, Q. Jiang, P. Xiao, J. Zou, Q. Li, H. Jiang, Deregulation of the planar cell polarity genes CELSR3 and FZD3 in Hirschsprung disease, Exp. Mol. Pathol. 101 (2) (2016) 241–248.
[134] H. Kondo, H. Hayashi, K. Oshima, T. Tahira, K. Hayashi, Frizzled 4 gene (FZD4) mutations in patients with familial exudative vitreoretinopathy with variable expressivity, Br. J. Ophthalmol. 87 (10) (2003) 1291–1295.

[135] J. Robitaille, M.L.E. MacDonald, A. Kaykas, L.C. Sheldahl, J. Zeisler, M.-P. Dubé, L.-H. Zhang, R.R. Singaraja, D.L. Guernsey, B. Zheng, L.F. Siebert, A. Hoskin-Mott, M.T. Trese, S.N. Pimstone, B.S. Shastry, R.T. Moon, M.R. Hayden, Y.P. Goldberg, M.E. Samuels, Mutant frizzled-4 disrupts retinal angiogenesis in familial exudative vitreoretinopathy, Nat. Genet. 32 (2) (2002) 326–330.
[136] C. Liu, S.A. Widen, K.A. Williamson, R. Ratnapriya, C. Gerth-Kahlert, J. Rainger, R.P. Alur, E. Strachan, S.H. Manjunath, A. Balakrishnan, J.A. Floyd, U. K. Consortium, T. Li, A. Waskiewicz, B.P. Brooks, O.J. Lehmann, D.R. FitzPatrick, A. Swaroop, A secreted WNT-ligand-binding domain of FZD5 generated by a frameshift mutation causes autosomal dominant coloboma, Hum. Mol. Genet. 25 (7) (2016) 1382–1391.
[137] P. De Marco, E. Merello, A. Rossi, G. Piatelli, A. Cama, Z. Kibar, V. Capra, FZD6 is a novel gene for human neural tube defects, Hum. Mutat. 33 (2) (2012) 384–390.
[138] C. Kasparis, D. Reid, N.J. Wilson, V. Okur, C. Cole, C.D. Hansen, K. Bosse, R. C. Betz, M. Khan, F.J. Smith, Isolated recessive nail dysplasia caused by FZD6 mutations: report of three families and review of the literature, Clin. Exp. Dermatol. 41 (8) (2016) 884–889.
[139] C. Saygi, Y. Alanay, U. Sezerman, A. Yenenler, N. Ozoren, A possible founder mutation in FZD6 gene in a Turkish family with autosomal recessive nail dysplasia, BMC Med. Genet. 20 (1) (2019) 15.
[140] E.M. Cherniske, T.O. Carpenter, C. Klaiman, E. Young, J. Bregman, K. Insogna, R. T. Schultz, B.R. Pober, Multisystem study of 20 older adults with Williams syndrome, Am. J. Med Genet Part A 131 (3) (2004) 255–264.
[141] C. Schubert, The genomic basis of the Williams-Beuren syndrome, Cell Mol. Life Sci. 66 (7) (2009) 1178–1197.
[142] B.R. Pober, Williams-Beuren syndrome, New Engl. J. Med. 362 (3) (2010) 239–252.
[143] A. Heilmann, T. Schinke, R. Bindl, T. Wehner, A. Rapp, M. Haffner-Luntzer, C. Nemitz, A. Liedert, M. Amling, A. Ignatius, The Wnt serpentine receptor Frizzled-9 regulates new bone formation in fracture healing, PLoS One 8 (12) (2013), e84232.
[144] J. White, J.F. Mazzeu, A. Hoischen, S.N. Jhangiani, T. Gambin, M.C. Alcino, S. Penney, J.M. Saraiva, H. Hove, F. Skovby, H. Kayserili, E. Estrella, A.T. Vulto-van Silfhout, M. Steehouwer, D.M. Muzny, V.R. Sutton, R.A. Gibbs, G. Baylor-Hopkins, Center for Mendelian, J.R. Lupski, H.G. Brunner, B.W. van Bon, C. M. Carvalho, DVL1 frameshift mutations clustering in the penultimate exon cause autosomal-dominant Robinow syndrome, Am. J. Hum. Genet. 96 (4) (2015) 612–622.
[145] K.J. Bunn, P. Daniel, H.S. Rosken, A.C. O'Neill, S.R. Cameron-Christie, T. Morgan, H.G. Brunner, A. Lai, H.P. Kunst, D.M. Markie, S.P. Robertson, Mutations in DVL1 cause an osteosclerotic form of Robinow syndrome, Am. J. Hum. Genet. 96 (4) (2015) 623–630.
[146] L. Liu, W. Liu, Y. Shi, L. Li, Y. Gao, Y. Lei, R. Finnell, T. Zhang, F. Zhang, L. Jin, H. Li, W. Tao, H. Wang, DVL mutations identified from human neural tube defects and Dandy-Walker malformation obstruct the Wnt signaling pathway, J. Genet. Genom. 47 (6) (2020) 301–310.
[147] J.J. White, J.F. Mazzeu, A. Hoischen, Y. Bayram, M. Withers, A. Gezdirici, V. Kimonis, M. Steehouwer, S.N. Jhangiani, D.M. Muzny, R.A. Gibbs, G. Baylor-Hopkins, Center for Mendelian, B.W.M. van Bon, V.R. Sutton, J.R. Lupski, H. G. Brunner, C.M.B. Carvalho, DVL3 alleles resulting in a -1 frameshift of the last exon mediate autosomal-dominant robinow syndrome, Am. J. Hum. Genet. 98 (3) (2016) 553–561.
[148] E.A. Otto, B. Schermer, T. Obara, J.F. O'Toole, K.S. Hiller, A.M. Mueller, R.G. Ruf, J. Hoefele, F. Beekmann, D. Landau, J.W. Foreman, J.A. Goodship, T. Strachan, A. Kispert, M.T. Wolf, M.F. Gagnadoux, H. Nivet, C. Antignac, G. Walz, I. A. Drummond, T. Benzing, F. Hildebrandt, Mutations in INVS encoding inversin cause nephronophthisis type 2, linking renal cystic disease to the function of primary cilia and left-right axis determination, Nat. Genet. 34 (4) (2003) 413–420.
[149] S. Bellavia, K. Dahan, S. Terryn, J.P. Cosyns, O. Devuyst, Y. Pirson, A homozygous mutation in INVS causing juvenile nephronophthisis with abnormal reactivity of the Wnt/beta-catenin pathway, Nephrol. Dial. Transpl. 25 (12) (2010) 4097–4102.
[150] E. Merello, S. Mascelli, A. Raso, G. Piatelli, A. Consales, A. Cama, Z. Kibar, V. Capra, P.D. Marco, Expanding the mutational spectrum associated to neural tube defects: literature revision and description of novel VANGL1 mutations, Birth Defects Res A Clin. Mol. Teratol. 103 (1) (2015) 51–61.
[151] Y.-P. Lei, T. Zhang, H. Li, B.-L. Wu, L. Jin, H.-Y. Wang, VANGL2 mutations in human cranial neural-tube defects, New Engl. J. Med. 362 (23) (2010) 2232–2235.
[152] A.G. Bassuk, R.H. Wallace, A. Buhr, A.R. Buller, Z. Afawi, M. Shimojo, S. Miyata, S. Chen, P. Gonzalez-Alegre, H.L. Griesbach, S. Wu, M. Nashelsky, E.K. Vladar, D. Antic, P.J. Ferguson, S. Cirak, T. Voit, M.P. Scott, J.D. Axelrod, C. Gurnett, A. S. Daoud, S. Kivity, M.Y. Neufeld, A. Mazarib, R. Straussberg, S. Walid, A. D. Korczyn, D.C. Slusarski, S.F. Berkovic, H.I. El-Shanti, A homozygous mutation in human PRICKLE1 causes an autosomal-recessive progressive myoclonus epilepsy-ataxia syndrome, Am. J. Hum. Genet. 83 (5) (2008) 572–581.
[153] H. Algahtani, F. Al-Hakami, M. Al-Shehri, B. Shirah, M.H. Al-Qahtani, A. A. Abdulkareem, M.I. Naseer, A very rare form of autosomal dominant progressive myoclonus epilepsy caused by a novel variant in the PRICKLE1 gene, Seizure 69 (2019) 133–139.
[154] M.L. Gonzalez-Garay, M.B. Aldrich, J.C. Rasmussen, R. Guilliod, P.E. Lapinski, P. D. King, E.M. Sevick-Muraca, A novel mutation in CELSR1 is associated with hereditary lymphedema, Vasc. Cell 8 (2016) 1.
[155] Y. Lei, H. Zhu, W. Yang, M.E. Ross, G.M. Shaw, R.H. Finnell, Identification of novel CELSR1 mutations in spina bifida, PLoS One 9 (3) (2014), e92207.
[156] R. Allache, P. De Marco, E. Merello, V. Capra, Z. Kibar, Role of the planar cell polarity gene CELSR1 in neural tube defects and caudal agenesis, Birth Defects Res. Part A Clin. Mol. Tertaol. 94 (3) (2012) 176–181.
[157] T. Vilboux, M.C. Malicdan, J.C. Roney, A.R. Cullinane, J. Stephen, D. Yildirimli, J. Bryant, R. Fischer, M. Vemulapalli, J.C. Mullikin, N.C.S. Program, P. J. Steinbach, W.A. Gahl, M. Gunay-Aygun, CELSR2, encoding a planar cell polarity protein, is a putative gene in Joubert syndrome with cortical heterotopia, microophthalmia, and growth hormone deficiency, Am. J. Med. Genet. A 173 (3) (2017) 661–666.
[158] S. Wang, J.D. Mandell, Y. Kumar, N. Sun, M.T. Morris, J. Arbelaez, C. Nasello, S. Dong, C. Duhn, X. Zhao, Z. Yang, S.S. Padmanabhuni, D. Yu, R.A. King, A. Dietrich, N. Khalifa, N. Dahl, A.Y. Huang, B.M. Neale, G. Coppola, C. A. Mathews, J.M. Scharf, S. Tourette, International Collaborative Genetics, S. Tourette Syndrome Genetics, I. Eastern Europe, G. Tourette Association of America International Consortium for, T.V. Fernandez, J.D. Buxbaum, S. De Rubeis, D.E. Grice, J. Xing, G.A. Heiman, J.A. Tischfield, P. Paschou, A. J. Willsey, M.W. State, De Novo sequence and copy number variants are strongly associated with Tourette Disorder and implicate cell polarity in pathogenesis, Cell Rep. 24 (13) (2018) 3441–3454 e12.
[159] N. Lahrouchi, A. George, I. Ratbi, R. Schneider, S.C. Elalaoui, S. Moosa, S. Bharti, R. Sharma, M. Abu-Asab, F. Onojafe, N. Adadi, E.M. Lodder, F.Z. Laarabi, Y. Lamsyah, H. Elorch, I. Chebbar, A.V. Postma, V. Lougaris, A. Plebani, J. Altmueller, H. Kyrieleis, V. Meiner, H. McNeill, K. Bharti, S. Lyonnet, B. Wollnik, A. Henrion-Caude, A. Berraho, F. Hildebrandt, C.R. Bezzina, B. P. Brooks, A. Sefiani, Homozygous frameshift mutations in FAT1 cause a syndrome characterized by colobomatous-microphthalmia, ptosis, nephropathy and syndactyly, Nat. Commun. 10 (1) (2019) 1180.
[160] M. Neumann, M. Seehawer, C. Schlee, S. Vosberg, S. Heesch, E.K. von der Heide, A. Graf, S. Krebs, H. Blum, N. Gokbuget, S. Schwartz, D. Hoelzer, P.A. Greif, C. D. Baldus, FAT1 expression and mutations in adult acute lymphoblastic leukemia, Blood Cancer J. 4 (2014), e224.
[161] H. Zhou, M. Xiao, X. Zhou, Y. Hao, C. Xin, Y. Tang, Y. Liang, Y. Zhang, S. Li, Aplastic anemia preceding acute lymphoblastic leukemia in an adult with FAT1 mutation, Minerva Med. 110 (6) (2019) 593–594.
[162] F. Puppo, E. Dionnet, M.-C. Gaillard, P. Gaildrat, C. Castro, C. Vovan, K. Bertaux, R. Bernard, S. Attarian, K. Goto, I. Nishino, Y. Hayashi, F. Magdinier, M. Krahn, F. Helmbacher, M. Bartoli, N. Lévy, Identification of variants in the 4q35 gene FAT1 in patients with a facioscapulohumeral dystrophy-like phenotype, Hum. Mutat. 36 (4) (2015) 443–453.
[163] G. Tate, K. Kishimoto, T. Mitsuya, A novel mutation of the FAT2 gene in spinal meningioma, Oncol. Lett. 12 (5) (2016) 3393–3396.
[164] D.C. Lin, J.J. Hao, Y. Nagata, L. Xu, L. Shang, X. Meng, Y. Sato, Y. Okuno, A. M. Varela, L.W. Ding, M. Garg, L.Z. Liu, H. Yang, D. Yin, Z.Z. Shi, Y.Y. Jiang, W. Y. Gu, T. Gong, Y. Zhang, X. Xu, O. Kalid, S. Shacham, S. Ogawa, M.R. Wang, H. P. Koeffler, Genomic and molecular characterization of esophageal squamous cell carcinoma, Nat. Genet. 46 (5) (2014) 467–473.
[165] K. Sato, N. Komune, T. Hongo, K. Koike, A. Niida, R. Uchi, T. Noda, R. Kogo, N. Matsumoto, H. Yamamoto, M. Masuda, Y. Oda, K. Mimori, T. Nakagawa, Genetic landscape of external auditory canal squamous cell carcinoma, Cancer Sci. 111 (8) (2020) 3010–3019.
[166] B. Luzon-Toro, H. Gui, M. Ruiz-Ferrer, C. Sze-Man Tang, R.M. Fernandez, P. C. Sham, A. Torroglosa, P. Kwong-Hang Tam, L. Espino-Paisan, S.S. Cherny, M. Bleda, V. Enguix-Riego Mdel, J. Dopazo, G. Antinolo, M.M. Garcia-Barcelo, S. Borrego, Exome sequencing reveals a high genetic heterogeneity on familial Hirschsprung disease, Sci. Rep. 5 (2015) 16473.
[167] M. Alders, L. Al-Gazali, I. Cordeiro, B. Dallapiccola, L. Garavelli, B. Tuysuz, F. Salehi, M.A. Haagmans, O.R. Mook, C.B. Majoie, M.M. Mannens, R. C. Hennekam, Hennekam syndrome can be caused by FAT4 mutations and be allelic to Van Maldergem syndrome, Hum. Genet. 133 (9) (2014) 1161–1167.
[168] S. Cappello, M.J. Gray, C. Badouel, S. Lange, M. Einsiedler, M. Srour, D. Chitayat, F.F. Hamdan, Z.A. Jenkins, T. Morgan, N. Preitner, T. Uster, J. Thomas, P. Shannon, V. Morrison, N. Di Donato, L. Van Maldergem, T. Neuhann, R. Newbury-Ecob, M. Swinkells, P. Terhal, L.C. Wilson, P.J.G. Zwijnenburg, A. J. Sutherland-Smith, M.A. Black, D. Markie, J.L. Michaud, M.A. Simpson, S. Mansour, H. McNeill, M. Götz, S.P. Robertson, Mutations in genes encoding the cadherin receptor-ligand pair DCHS1 and FAT4 disrupt cerebral cortical development, Nat. Genet. 45 (11) (2013) 1300–1308.
[169] R. Durst, K. Sauls, D.S. Peal, A. deVlaming, K. Toomer, M. Leyne, M. Salani, M. E. Talkowski, H. Brand, M. Perrocheau, C. Simpson, C. Jett, M.R. Stone, F. Charles, C. Chiang, S.N. Lynch, N. Bouatia-Naji, F.N. Delling, L.A. Freed, C. Tribouilloy, T. Le Tourneau, H. LeMarec, L. Fernandez-Friera, J. Solis, D. Trujillano, S. Ossowski, X. Estivill, C. Dina, P. Bruneval, A. Chester, J.J. Schott, K.D. Irvine, Y. Mao, A. Wessels, T. Motiwala, M. Puceat, Y. Tsukasaki, D. R. Menick, H. Kasiganesan, X. Nie, A.M. Broome, K. Williams, A. Johnson, R. R. Markwald, X. Jeunemaitre, A. Hagege, R.A. Levine, D.J. Milan, R.A. Norris, S. A. Slaugenhaupt, Mutations in DCHS1 cause mitral valve prolapse, Nature 525 (7567) (2015) 109–113.
[170] A. Clemenceau, J.C. Berube, P. Belanger, N. Gaudreault, M. Lamontagne, O. Toubal, M.A. Clavel, R. Capoulade, P. Mathieu, P. Pibarot, Y. Bosse,

Deleterious variants in DCHS1 are prevalent in sporadic cases of mitral valve prolapse, Mol. Genet. Genom. Med. 6 (1) (2018) 114–120.
[171] T. Le Tourneau, J. Merot, A. Rimbert, S. Le Scouarnec, V. Probst, H. Le Marec, R. A. Levine, J.J. Schott, Genetics of syndromic and non-syndromic mitral valve prolapse, Heart 104 (12) (2018) 978–984.
[172] C.H. An, E.M. Je, N.J. Yoo, S.H. Lee, Frameshift mutations of cadherin genes DCHS2, CDH10 and CDH24 genes in gastric and colorectal cancers with high microsatellite instability, Pathol. Oncol. Res. 21 (1) (2015) 181–185.